COMILLAS
UNIVERSIDAD PONTIFICIA
ICAI

GRADO EN INGENIERÍA EN TECNOLOGÍAS INDUSTRIALES

TRABAJO FIN DE GRADO

DEVELOPMENT OF A PSS/E TOOL FOR SIMULATING MULTIPLE HIGH VOLTAGE DIRECT CURRENT MULTI-TERMINAL LINKS WITH VOLTAGE SOURCE CONVERTERS

Autor: Carlos Prieto Rodríguez de Vera

Director: Luis Rouco Rodríguez

Co-Director: Lukas Sigrist

Madrid

Agosto de 2023

Carlos Prieto Rodríguez de Vera, declara bajo su responsabilidad, que el Proyecto con título **Development a PSS/E tool for Simulating Multiple High Voltage Direct Current Multi-Terminal links with Voltage Source Converters** presentado en la ETS de Ingeniería (ICAI) de la Universidad Pontificia Comillas en el curso académico 2022/23 es de su autoría, original e inédito y no ha sido presentado con anterioridad a otros efectos. El Proyecto no es plagio de otro, ni total ni parcialmente y la información que ha sido tomada de otros documentos está debidamente referenciada.

Fdo.: ..... Fecha: 30 / 08 / 2023

Autoriza la entrega:

El Director del Proyecto

Dr. Luis Rouco Rodríguez

Fdo.: ..... Fecha: 30 / 08 / 2023

COMILLAS
UNIVERSIDAD PONTIFICIA
ICAI

GRADO EN INGENIERÍA EN TECNOLOGÍAS INDUSTRIALES

TRABAJO FIN DE GRADO

DEVELOPMENT OF A PSS/E TOOL FOR SIMULATING MULTIPLE HIGH VOLTAGE DIRECT CURRENT MULTI-TERMINAL LINKS WITH VOLTAGE SOURCE CONVERTERS

Autor: Carlos Prieto Rodríguez de Vera

Director: Luis Rouco Rodríguez

Co-Director: Lukas Sigrist

Madrid

Agosto de 2023

Resumen

Development of a PSS/E tool for Simulating Multiple High Voltage Direct Current Multi-Terminal links with Voltage Source Converters.

Autor: **Prieto Rodríguez de Vera, Carlos.**

Director: Rouco Rodríguez, Luis.

Co-Director: Sigrist, Lukas

Entidad Colaboradora: ICAI – Universidad Pontificia Comillas.

Resumen Del Proyecto

El tema de este trabajo son los enlaces de Corriente Continua de Alto Voltaje (HVDC por sus siglas en inglés) con convertidores de fuente de tensión (VSC), una tecnología que presenta ventajas únicas y una reducción de costes para transmisiones de largo alcance, Figura 1.

Además, las ventajas más notables del uso de enlaces HVDC son los mencionados a continuación. Mayor capacidad de transporte de potencia con un menor derecho de vía comparado con Alterna de Alta Tensión (HVAC). Esto se debe a la reducción de pérdidas en transmisiones de largo alcance causadas por el efecto piel y a la componente reactiva en alterna. Los enlaces HVDC también permiten la conexión asíncrona, es decir el enlace eléctrico de áreas de distinta frecuencia. Un ejemplo de ello es la presa hidroeléctrica de Itaipu, conectando una generación de 50Hz con un consumo en Brasil a 60Hz.

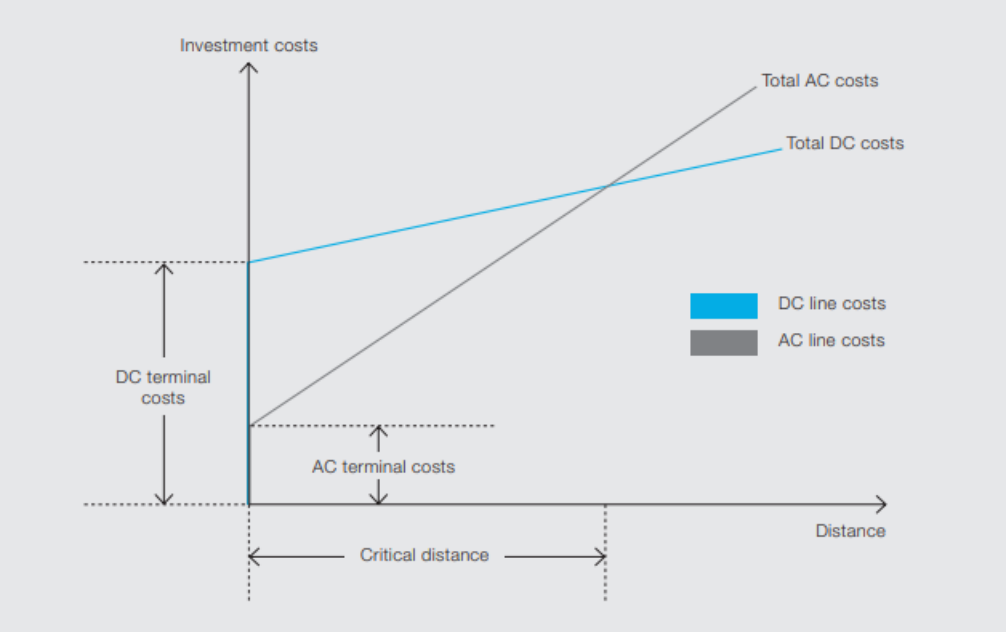

Figura 1: Gráfico de costes contra distancia de transmisión

Los enlaces HVDC se introdujeron al mercado en 1954 con el proyecto Gotland, desde entonces han sido mejorados considerablemente. Ahora, las redes HVDC-VSC Multi-Terminales no son solo viables, sino que se están convirtiendo en una solución interesante para algunas transmisiones. un ejemplo de ello es la interconexión de los parques eólicos marinos del mar del norte.

Un elemento clave de un enlace HVDC es el convertidor. El primer convertidor utilizado se basaba en válvulas de arco de mercurio, cuyo comportamiento era difícil de predecir y requería un mantenimiento laborioso y frecuente. Luego se inventaron las válvulas basadas en tiristores usadas en convertidores LCC. Estas eran una mejora respecto a las válvulas anteriores, pero aún tenían algunos problemas. El desarrollo más reciente son los convertidores VSC, que utilizan interruptores IGBT. Permiten altas impedancias de red, son capaces de generar y consumir energía reactiva y no requieren filtros armónicos. Todas estas son mejoras en comparación con los LCC, pero a un coste ligeramente más alto, aunque esta diferencia de precio disminuye.

A pesar de ello, en estos momentos no existe ningún programa de simulación de flujos, como PSS/E, con la capacidad de simular redes HVDC-VSC Multi-Terminales. El IIT posee un modelo de simulación de un enlace Multi-Terminal [1]. Actualmente, existe un interés industrial en crear un modelo capaz de simular diversas redes HVDC-VSC Multi-Terminales simultáneamente. Por ello, el objetivo

de este trabajo ha sido la ampliación del modelo del IIT para lograr simular una multitud de estas redes.

Este trabajo tiene dos partes, la solución estática en la operación de un sistema de energía y la simulación dinámica de una perturbación.

Para la expansión del modelo de simulación estática y a fin de permitir una multitud de redes CC, la metodología seguida ha sido la siguiente. En primer lugar, se estudiaron los modelos matemáticos del IIT actuales para los convertidores y las simulaciones de flujo de potencia. Luego, se modificó la gestión de datos del modelo para permitir la entrada del usuario de varias redes y el correcto uso de las funciones con las nuevas características de múltiples redes. Finalmente, se adaptaron los criterios de convergencia para tener esto en cuenta.

Para la expansión del modelo dinámico, se siguieron los siguientes pasos. En primer lugar, se creó un archivo principal en Python capaz de gestionar la simulación dinámica. Se vinculó este archivo al modelo original para conectar las salidas estáticas con las entradas dinámicas. Posteriormente se crearon funciones de automatización para crear el archivo DYR, responsable de conectar los parámetros definidos por el usuario con los modelos Fortran a través de PSS/E. A continuación se modificaron los modelos de convertidores Fortran para tener en cuenta la existencia de múltiples redes en la simulación. Se corrigieron las salidas estáticas para ser utilizadas correctamente por los modelos Fortran, permitiendo la distinción de las redes en los archivos de salida. Se creó un código para simular una falta dinámica definida por el usuario, junto con un archivo de salida para la visualización, finalmente se conectaron estos al archivo Python principal.

Concluidas estas modificaciones, la expansión del modelo del IIT a un sistema con múltiples redes HVDC-VSC multi-terminales se ha logrado con éxito, pese a las dificultades encontradas. Con la ayuda de un ejemplo ilustrativo, se demostrará la capacidad de esta nueva herramienta. El ejemplo ilustrativo es la conexión de 2 redes HVDC-VSC multi-terminales al sistema Kundur [2] en los nudos 5, 7 y 11 para la primera red y 6, 8 y 10 para la segunda red, Figura 2.

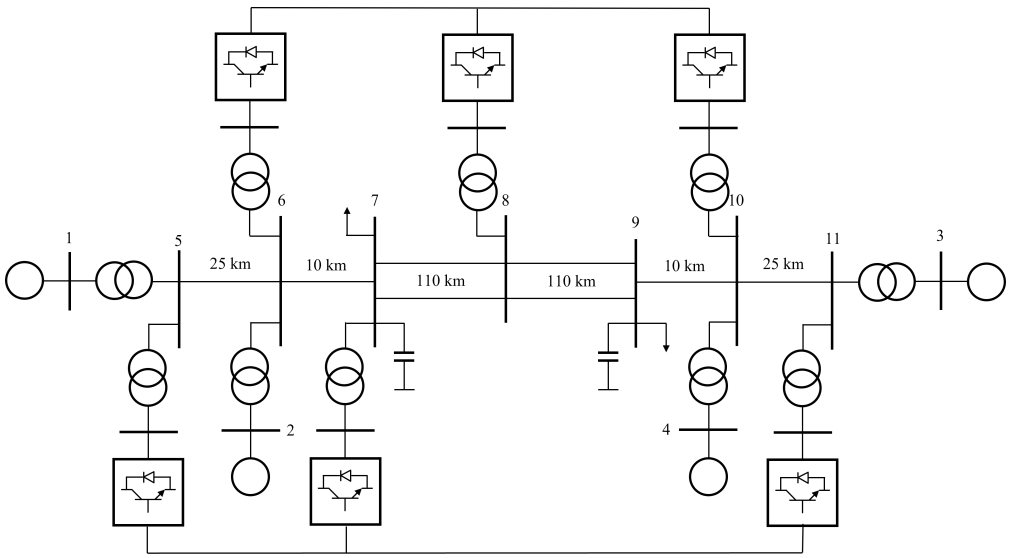

Figura 2: Sistema Kundur con 2 redes HVDC-VSC Multi-Terminales

La siguiente tabla es uno de los resultados principales de la simulación estática. Proporciona un resumen en el lado de continua de la red.

dcbus	**dctype1**	**dctype2**	**us (p.u)**	**delta_s (deg)**	**Ps (MW)**	**Qs (Mvar)**	**udc (p.u)**	**Pdc (MW)**
1	2	1	1,0139	6,89	−100,11	0,00	1,0000	96,69
2	1	1	0,9874	−8,52	45,00	0,00	0,9950	−47,83
3	1	1	1,0100	−6,63	45,00	0,00	0,9837	−47,83
4	2	1	0,9948	−1,58	−100,45	0,00	1,0000	97,20
5	1	1	0,9848	−16,80	45,00	0,00	0,9849	−47,79
6	1	1	0,9889	−17,61	45,00	0,00	0,9819	−47,79

Cuadro 1: Datos de la red HVDC para cada nudo

Las Figuras 3, 4 y 5 proporcionan algunos de los gráficos más notables producidos en la simulación dinámica de una falta en el nudo 9 de 100 ms.

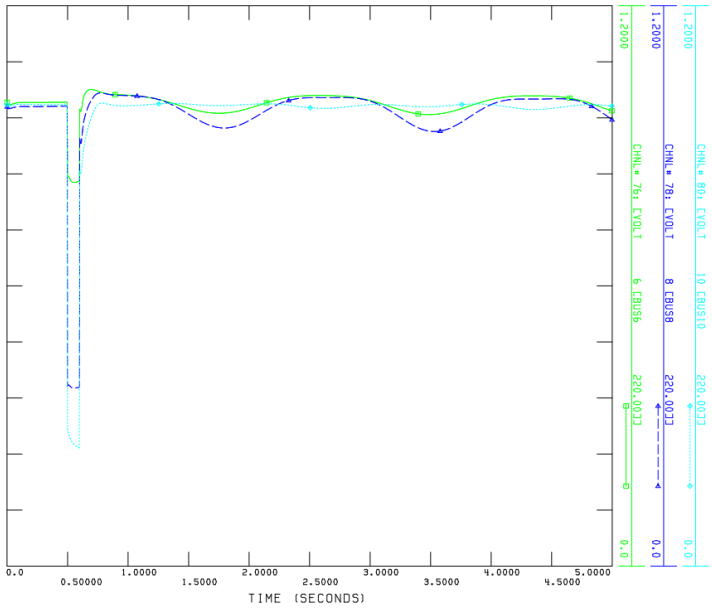

Figura 3: Tensión de los convertidores en los nudos 6, 8 y 10 - Red 1

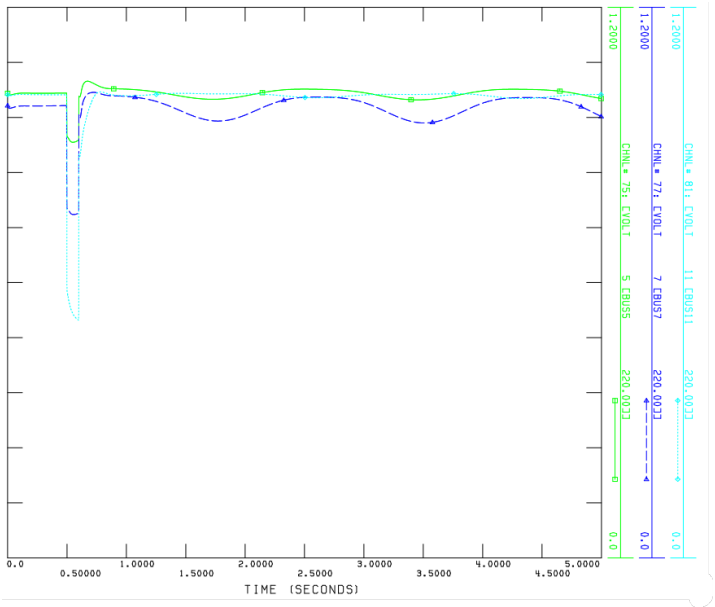

Figura 4: Tensión de los convertidores en los nudos 5, 7 y 11 - Red 2

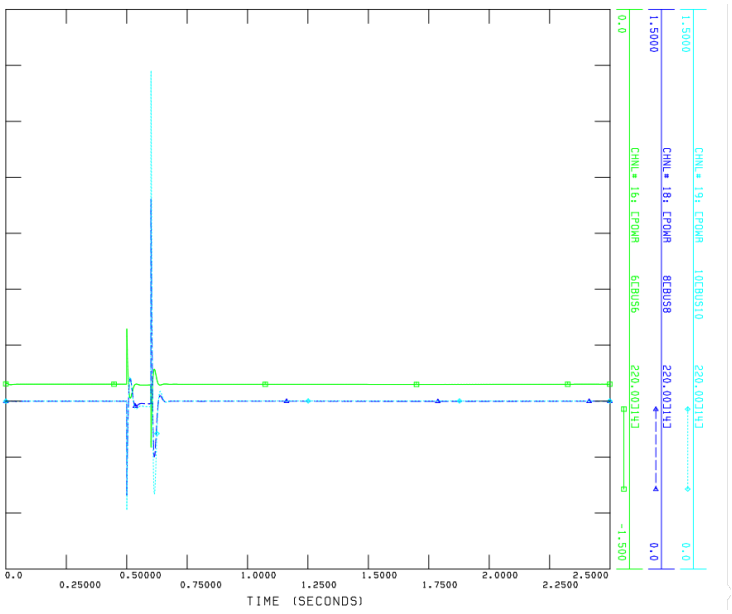

Figura 5: Potencia activa en los nudos 6, 8 y 10 - Red 1

Como era de esperar, el cambio en las nudos más cercanas a la falta es mayor que en los que están más alejadas de la ella. Se observa que los valores vuelven satisfactoriamente a unos valores aceptables en un corto período de tiempo.

El modelo se ha adaptado con éxito para la simulación de múltiples redes HVDC-VSC multi-terminales. Sin embargo, no está exento de limitaciones. Como en cualquier herramienta de flujo de potencia, la convergencia no está garantizada y depende de las condiciones iniciales. Los generadores equivalentes HVDC están modelados con un '14' como identificador, este número es fijo en el código y debería poder ser definido por el usuario. La versión de PSS/E empleada también limitará la capacidad de este modelo. Algunas modificaciones en el futuro deberían minimizar el alcance de estas limitaciones.

Con esta herramienta, se pueden realizar otros estudios. Algunos estudios interesantes podrían ser el análisis, desde un punto de vista económico, de las ventajas de expandir enlaces HVDC simples a multi-terminales o la viabilidad económica de algunos proyectos propuestos, como la red HVDC del Mar del Norte o la 'Supergrid' europea.

Figura 6: Possible North Sea HVDC grid as invisioned by ABB [3]

Development of a PSS/E tool for Simulating Multiple High Voltage Direct Current Multi-Terminal links with Voltage Source Converters.

Author: **Prieto Rodríguez de Vera, Carlos**

Director: Rouco Rodríguez, Luis

Co-Director: Sigrist, Lukas

Collaborating Entity: ICAI – Universidad Pontificia Comillas.

Summary of the Project

The topic of the work is High Voltage Direct Current links with voltage source converters, a technology that presents unique advantages and a cost reduction for long distance transmissions, Figure 7.

In addition, the most notable advantages of HVDC links are the following. Higher energy transmission capacity with a lower rights of way compared with HVAC. This is due to the reduction in power losses for long transmissions caused by the skin effect and the reactive component of alternating currents. Also, HVDC provides the ability of asynchronous connections, meaning regions of different frequencies can be linked electrically. An example of this being the Itaipu hydroelectric dam connection from 50Hz generation to a 60Hz Brazilian consumption.

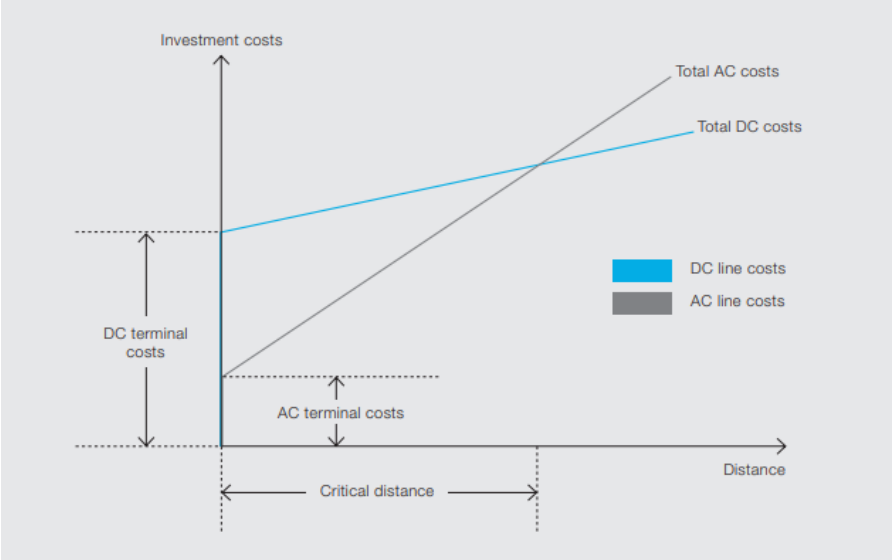

Figure 7: Cost vs distance of transmission graph [4]

HVDC was introduced to the market in 1954 with the Gotland project, and has since been improved massively. Up to a point where Multi-Terminal HVDC-VSC grids are not only viable, but are becoming an interesting solution for certain transmissions. One such example is the interconnection of the North Sea's offshore wind farms.

One key element of an HVDC link is the converter. The first converter used was based on mercury arc valves, their behaviour was difficultly predicted and the maintenance was laborious and frequent. Then thyristor based valves were invented and used in LCC converters. These improved upon the previous valves but still had some issues. The most recent development are VSC converters, that use IGBT switches. Allowing high grid impedances, are capable of both producing and consuming reactive power and do not require harmonic filters. All improvements when compared with LCC, but, at a slightly higher cost, although this gap is closing.

Despite this, currently no power flow tool, such as PSS/E, offers simulation capabilities for Multi-Terminal HVDC-VSC grids. IIT has a model capable of simulating a single Multi-Terminal link [1]. Nevertheless, there is an industrial desire to create a model capable of simulating multiple Multi-Terminal HVDC-VSC grids simultaneously. Therefore, the objective of this work has been the expansion of the IIT model to simulate several of these grids.

This work deals with 2 main parts, the steady-state solution of a power system

operating point and with the dynamic simulation of a disturbance.

For the expansion of the steady-state simulation model to allow for a multitude of DC grids, the methodology followed has been the following. Firstly the understanding of the current IIT mathematical models of the converters and power flow simulations. Then the modification of the data management in the model to allow for user input of several grids and the correct use of the functions with the new multi grid characteristics. Followed by an adaptation of the convergence criteria to take this into account.

For the expansion of the dynamic model, these were the steps taken. Firstly the creation of a main Python file capable of managing the dynamic simulation and linking this file to the previous model to connect the steady-state outputs with the dynamic inputs. Create the automation functions to create the DYR file, responsible of connecting the user defined parameters with the Fortran models via PSS/E. Modify the Fortran converter models to take into account the new multi grid aspect of the simulation. Modify the steady-state outputs to properly be used by the Fortran models, allowing for grid distinctions in the output files. Create a dynamic fault code to simulate the user defined dynamic case, alongside an output file for visualization, and then connecting these to the base Python file.

Post this, the expansion of IIT's model to a system with multiple Multi-Terminal HVDC-VSC grids has been successfully, despite the difficulties encountered. With the help of an illustrative example this new tool is demonstrated. The illustrative example is the connection of 2 Multi-Terminal HVDC-VSC grids to the Kundur system [2] at buses 5,7 and 11 for the first grid and 6,8 and 10 for the second grid, Figure 8.

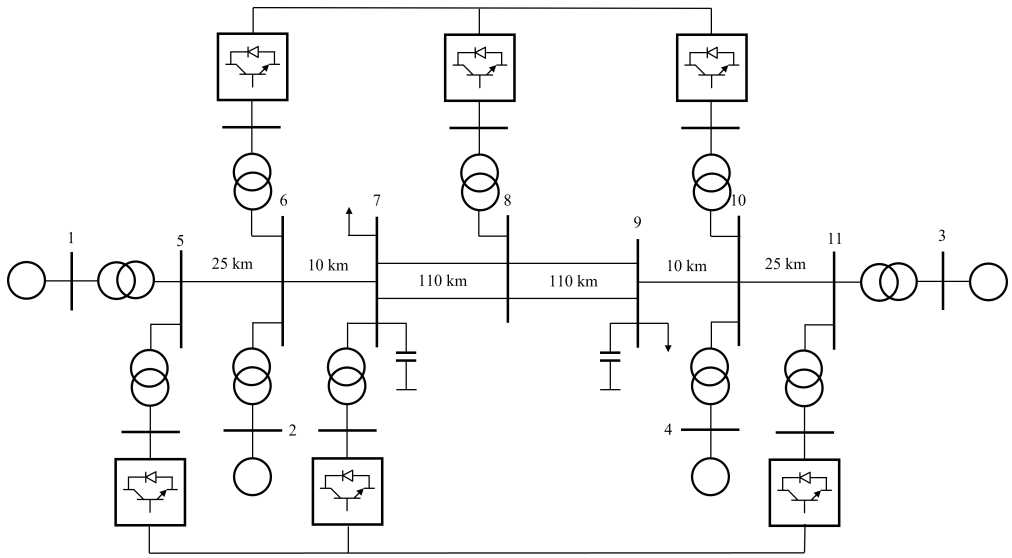

Figure 8: Kundur System with 2 Multi-Terminal HVDC-VSC grids

The next table shows one of the main steady-state results. It provides a summary of the DC side of the grid.

dcbus	**dctype1**	**dctype2**	**us (p.u)**	**delta_s (deg)**	**Ps (MW)**	**Qs (Mvar)**	**udc (p.u)**	**Pdc (MW)**
1	2	1	1.0139	6.89	−100.11	0.00	1.0000	96.69
2	1	1	0.9874	−8.52	45.00	0.00	0.9950	−47.83
3	1	1	1.0100	−6.63	45.00	0.00	0.9837	−47.83
4	2	1	0.9948	−1.58	−100.45	0.00	1.0000	97.20
5	1	1	0.9848	−16.80	45.00	0.00	0.9849	−47.79
6	1	1	0.9889	−17.61	45.00	0.00	0.9819	−47.79

Table 2: DC grid data for each bus

Figures 9, 10 and 11, provide some of the most notable graphs produced after the dynamic simulation of a bus fault of 100ms on bus 9.

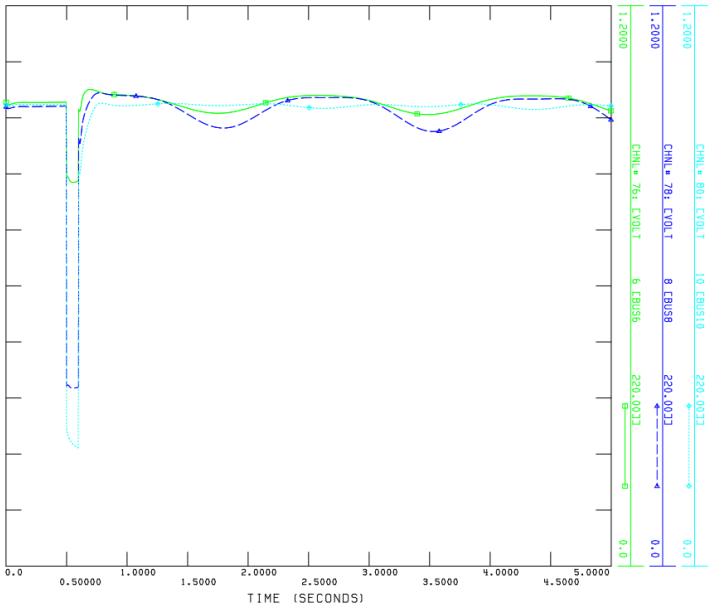

Figure 9: Voltage of converters at buses 6, 8 and 10 - Grid 1

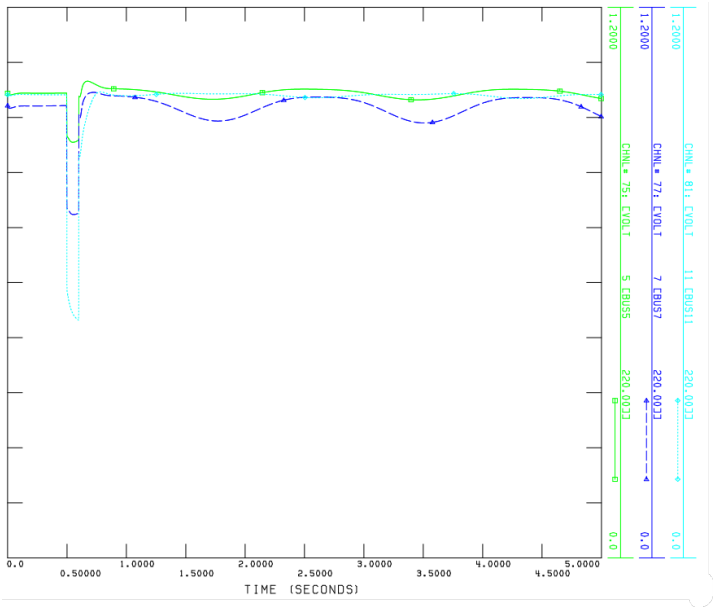

Figure 10: Voltage of converters at buses 5, 7 and 11 - Grid 2

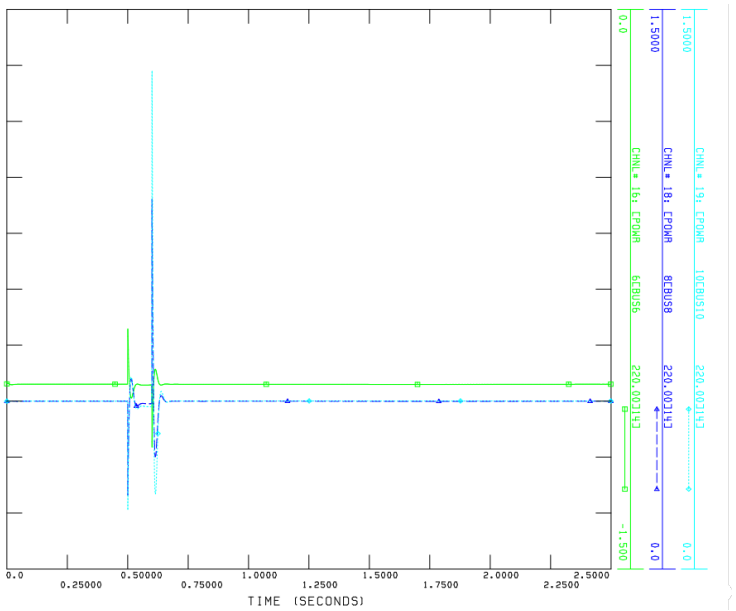

Figure 11: Active Power at buses 6, 8 and 10 - Grid 1

As expected, the change for the buses closer to the fault are larger than those further away from the fault. It is observed that the valuer return to acceptable values satisfactorily on a short period of time.

The model has been successfully adapted for the simulation of multiple Multi-Terminal HVDC-VSC grids. But not without some limitations. As in any power flow tool, convergence is not granted and depends on initial conditions. The HVDC equivalent generators are modeled with a '14' as the identifier, this number is hard-coded and should be user defined. The PSS/E version in use will also limit the capability of this model. Some modifications in the future should minimize the extent of these limitations.

With this tool other studies can now be performed. Some such studies that could be interesting could be analysing, cost wise, the advantages of expanding simple HVDC links to Multi-Terminals or the economic feasibility of some proposed projects such as North Sea HVDC grid or a European Supergrid.

Figure 12: Possible North Sea HVDC grid as invisioned by ABB [3]

Planning is indispensable,
plans are useless.
Dwight D. Eisenhower

Acknowledgements

I would like to express my sincere gratitude to the following individuals and organizations who have contributed to the completion of this project:

- Project Director, Dr. Luis Rouco Rodríguez, for his invaluable guidance, support, and mentorship throughout this research. Also for the opportunity to work on this project. Alfso for all the international meetings at unusual hours to cope with the time difference.
- Project Co-Director, Dr. Lukas Sigrist, for the thorough help understanding the different programming languages, the help going through the IIT models and the long meetings to figure out solutions to the challenges that seemed non ending.
- IIT, for their technical support with the required tools for the completion of this work.
- My family for their unwavering encouragement and understanding during this journey.

I am deeply thankful for the collective effort and encouragement that have made this project a reality.

Contents

List of Figures

List of Tables

Acronyms

ICAI	Insitituto Católico de Artes e Industrias
IIT	Insitituto de Investigación Tecnológica
PFC	Proyecto Fin de Carrera
HVDC	High Voltage Direct Current
MTDC	Multi-Terminal Direct Current
VSC	Voltage Source Converters
LCC	Line Commutated Converters
PSS/E	Power System Simulation for Engineers
ODS	Objetivos de Desarrollo Sostenible
SDG	Sustainable Development Goals
IVF	Intel Visual Fortran compiler
DLL	Dynamic Link Library
TXT	Text file
POD	Power Oscillation Damping
POM	Program Operations Manual
API	Application Program Interface
ASEA	General Swedish Electric Company
XLPE	Cross-linked polyethylene
IGBT	Insulated-Gate Bipolar Transistor

Chapter 1

Introduction

This introductory chapter aims to explain the topics discussed in this thesis. Starting with the actual topic of the work, following with the objectives and motivations all the way to discussing the organisation of the document.

1.1 The topic of the work

The topic of this work is High Voltage Direct Current (HVDC) transmission. HVDC has become a mature technology with a broad set of applications. Among them, we can highlight the transmission of bulk power from remote generation, alleviation of congested corridors, underwater and underground transmission, connecting systems of different frequencies, and asynchronous connection of large interconnected systems [5]. Therefore, these links could help with the rapid inclusion of renewable sources into the system whilst adding an extra layer of stability.

Two HVDC technologies can be found: HVDC based on Line Commutated Converters or HVDC-LCC (that make use of thyristor switches) and HVDC based on Voltage Source Converters or HVDC-VSC (that make use of IGBT switches).

The milestone on the development of HVDC transmission was when ASEA commissioned in 1954 the first commercial HVDC link in the world (20 MW, 100 kV Gotland). The converter valves were mercury-arc valves.

HVDC-LCC needs low grid impedance (high short circuit capacity) at the connection point, consumes reactive power, and needs harmonic filters. HVDC-VSC can work with high grid impedance (low short circuit capacity) at the connection

point, can either consume or produce reactive power, and does not need harmonic filters.

The development of multi-terminal HVDC transmission has been prevented by the lack of DC circuit breakers. Only some examples of multi-terminal HVDC transmission can be found. The most remarkable one is the multi-terminal HVDC-LCC Quebec-New England-New York, upgraded to multi-terminal by Hitachi Energy in 2013.

The massive development of offshore wind generation in the North Sea is driving the research and development of multi-terminal HVDC transmission using VSC technology.

The application of HVDC technology requires the steady-state and dynamic simulation of electric power systems. Most power system packages offer simulation tools and models of point-to-point HVDC links. In contrast, no simulation tools and models of multi-terminal HVDC-VSC links are available in power system packages.

IIT has already developed a PSS/E model of a multi-terminal HVDC-VSC link, building upon on the work and studies of Dr. Francisco Javier Renedo Anglada, an IIT researcher [1]. It is from this model and former mathematical formulas [6] from where this thesis stems. The model has two main components: the steady-state solution (power flow) and the dynamic simulation model of the converters and the DC link.

However, such a model can only handle one multi-terminal HVDC-VSC link. IIT has received requests for models with several multi-terminals in a system. Precisely, the connection to the grid of offshore wind generation in the coast of California would require several multi-terminal HVDC links.

As previously discussed, there are several scenarios where the deployment of VSC HVDC multi-terminal grids makes sense and would constitute an improvement. However, preceding physical implementation, a simulation tool has to be used and therefore, developed.

During this project such a tool will be developed. Alongside the model, a user manual will be included. As mentioned in the title, the model will simulate the inclusion of several Multi-Terminal HVDC grid, with VSC converters, into an AC grid on the power flow simulation program, PSS/E. For a better understanding of such grids and converters an entire chapter is devoted on the theory of HVDC Multi-Terminal VSC grids, Chapter 2.3.

The motivation behind this thesis lies in addressing the existing gaps in HVDC

Multi-Terminal simulation capabilities. Currently, there is a lack of simulation tools for multiple VSC-HVDC Multi-Terminal grids. The absence of such tools limits researchers, engineers, and system operators from accurately modeling and analysing the intricate behavior of these systems. This gap is, at least partially, responsible for the limited deployment of such grids, combined with the possible advantages they offer, the utility and appeal of this work is amplified.

The significance of this work extends beyond theoretical research. The practical applications of this more complete PSS/E tool will enable power system operators and planners to optimize the design and operation of VSC-HVDC Multi-Terminal grids. Leading to improved grid performance, enhanced stability, and ultimately, more reliable and sustainable electricity supply. This research intends to contribute in the advancement of VSC-HVDC simulation technology, supporting the global transition towards a cleaner and more resilient energy future. [1]

1.2 Objectives of the work

The two main activities are:

1. Extension of the power flow solution of Multi-Terminal HVDC systems to handle several systems
2. Extension of the dynamic simulation of Multi-Terminal HVDC systems to handle several systems

A secondary objective is the generation of a user manual alongside this new model, to simplify future use of the tool.

The implications of the first objective is that the prior model has to be adapted as solving a multitude of grids will affect both the convergence's main loop structure and its stopping criteria. As now each DC grid has to be solved prior to the solving of the AC grid.

The implications of the second objective is the need for a new python model that combines the steady-state model and a newly created dynamic model, into one single PSS/E model. Increasing automation and minimising the required user interface. Also, there has to be a new link between both models and between the dynamic model and the Power Flow tool, PSS/E, as the previous one becomes obsolete when introducing several grids. The dynamic models must be altered to

[1] Appendix A and Chapters 2.3, 2.4 extend on other factors influencing the motivation for this project such as SDG's and industrial needs.

solve the inter-model communications and a new automatic linking file creation function must be developed to solve the model - PSS/E communications.

1.3 Methods and tools

This work deals with the steady-state solution of a power system operating point and with the dynamic simulation of a disturbance.

The steady-state solution of a power system is provided by the so-called power flow solution. When a Multi-Terminal HVDC link is embedded in an AC power system, the power flow solution requires the solution of two grids: the AC and the DC ones. In the case of several multi-terminal HVDC links, the power flow solution will require the solution of the AC grid and the solution of the DC grid corresponding to each HVDC link.

The dynamic simulation of a power system consists of the numerical integration of the non-linear differential equations that describe the power system model. Simulating a Multi-Terminal HVDC link requires incorporating models of the DC grid and the converter controls. Simulating several multi-terminal HVDC links will require the ability of incorporating many models of the DC grid as Multi-Terminals and the models of the converters associated to each DC grid.

The tools required for this work are PSS/E, Python and Fortran. Python acts as a linking program as well as solving the DC power flow, which is then introduced in PSS/E for the AC solution and later convergence. For the dynamic model, the static results act as the initial conditions. Then, PSS/E is deployed for the dynamic simulation which uses the Fortran defined converter models and the Python defined parameters.

1.4 Organisation of the document

Following the current introductory chapter, Chapter 2 describes the technology of Multi-Terminal HVDC-VSC systems. Chapter 3 details the steady-state analysis of Multi-Terminal HVDC-VSC systems with PSS/E. Chapter 4 describes the dynamic analysis of Multi-Terminal HVDC-VSC systems with PSS/E. Chapter 5 contains an illustrative example. Chapter 6 provides the conclusions of the work.

Chapter 2

Multi-terminal HVDC systems

As an introduction on the grids studied the following will be said. HVDC lines are used for long distances or underwater links as it reduces the electric losses, several electric grid stakeholders have mentioned on the usefulness of expanding these links into grids for better grid stability and to help with a massive introduction of renewable sources into the grid.

2.1 HVDC transmissions

The first power system built by Edison around Pearl Street station was a Direct Current (DC) one. However, Edison's DC-based technology was superseded by Tesla and Westinghouse's alternating current-based technology due to its ability to transmit power over long distances at high voltage.

The invention of mercury arc valves and subsequently thyristors able to handle high voltages and high currents made possible the development of High Voltage Direct Current (HVDC) transmission.

HVDC transmission has proven less costly when transmitting large amounts of power over long distances.

Alternating Current (AC) transmission comprises the AC transmission line and the substation equipment (breakers, switches, instrument transformers, arresters, protection, control, and communication system) to connect the AC line to the system. DC transmission comprises the DC line and the converter stations. Of course, substation equipment is also needed to connect the converter stations to the system.

Figure 2.1, compares the cost of overhead AC and DC transmission as a function of the distance between the exporting and the importing areas. The cost of transmission at zero distance corresponds to the substation equipment of AC transmission and to the converter stations and associated substation equipment of DC transmission. The cost of AC transmission without compensation at zero distance is much lower than that of DC transmission due to the high cost of the converter stations. In contrast, the slope of the cost function of DC transmission is lower than the slope of the cost function of AC transmission since AC makes use of three conductors (three phases) whereas DC only makes use of two conductors (positive and negative). The crossing of the cost function of AC and DC transmission determines a breakeven distance from which the overall cost of DC transmission would be lower than the cost of AC transmission. It must be noted that AC transmission at very long distances may need shunt and series compensation which affects the cost function AC transmission as a function of the distance.

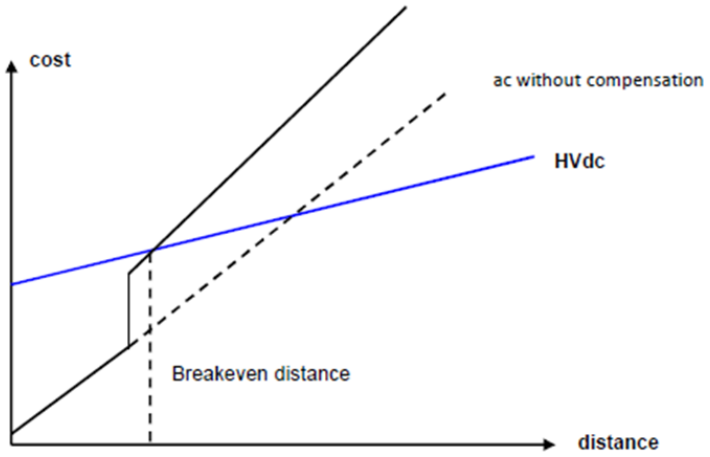

Figure 2.1: Cost comparison of overhead AC and DC as a function of distance.

In addition to cost advantage, DC transmission requires narrower rights of way that AC transmission as shown in Figure 2.2.

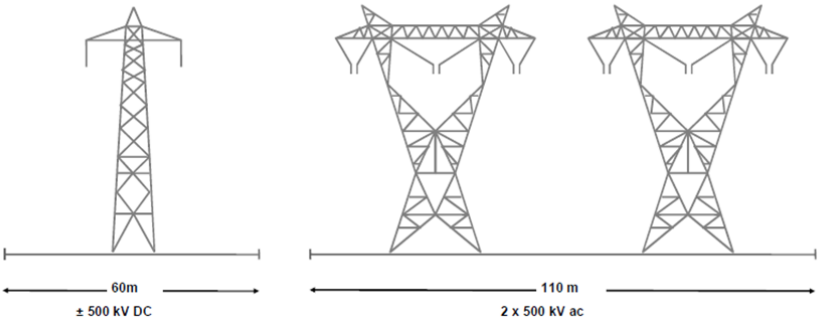

Figure 2.2: Rights of way of AC and DC transmission.

There is also a point to be made for HVDC lines for long distances as at longer ranges the losses are smaller to those compared with AC. Also, the capacity of both underground cables and overhead cables is less limited. the next plots compare the performance of HVAC vs HVDC when analysed over transmission distance. These aspects are displayed in Figures: 2.3, 2.4 and 2.5.

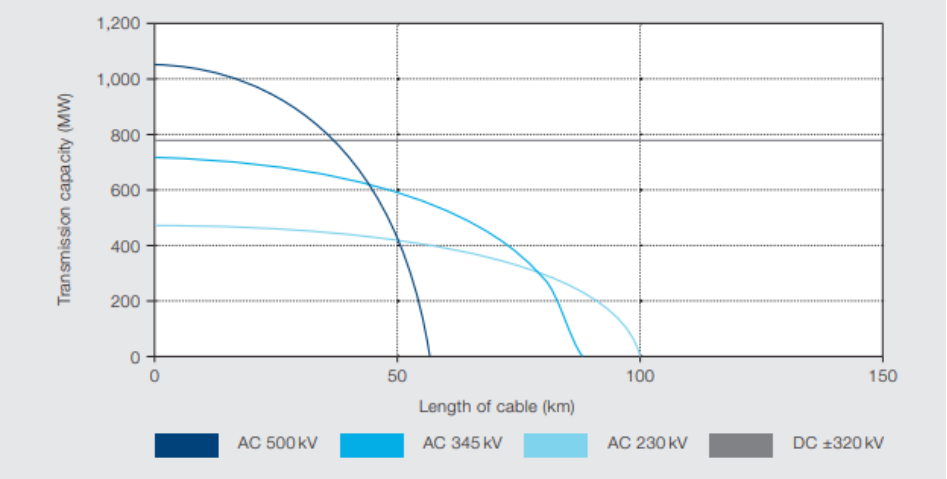

Figure 2.3: Transmission capacity of AC and DC with underground cables [4]

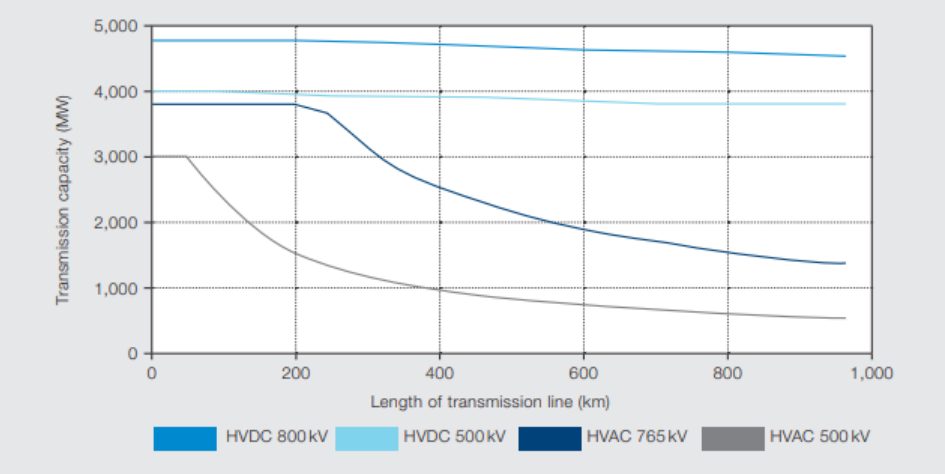

Figure 2.4: Transmission capacity of AC and DC with overhead cables [4]

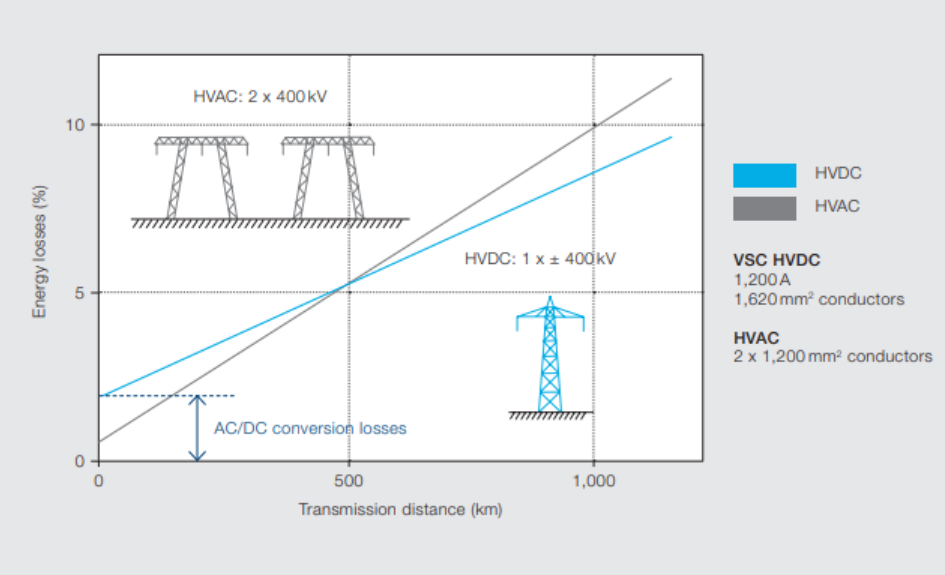

Figure 2.5: Losses as a percentage over transmission distance for HVAC and VSC - HVDC [4]

China is probably the best example of using HVDC transmission to transmit large amounts of power over long distances. Figure 2.6 shows the HVDC links in China.

The length of underground or undersea AC transmission is also limited due to the charging (capacitive) current of the cables. Table 2.1 provides the charging currents of 500 kV XLPE land cables of different sections and ampacity. It clearly

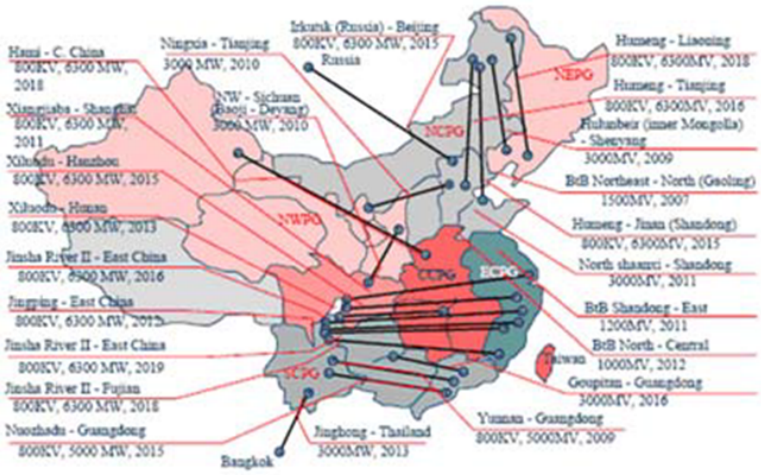

Figure 2.6: HVDC transmission of large amount of power over long distances in China.

shows that the charging current of a 100 km long cable would be greater than the current rating. More complex analysis of voltage regulation could impose harder constraints.

Cross section (mm2)	Current rating (A)	Charging current (A/km)
800	870	12.3
1000	960	13.7
1200	1115	15.1
1400	1205	15.9
1600	1280	16.6
2000	1410	17.6
2500	1540	19.2

Table 2.1: Charging currents of 500 kV XLPE land cables of different sections and ampacity.

It must be noted that the first commercial HVDC link in the world (20 MW, 100 kV) put in service in 1954 was an undersea link between mainland Sweden and Gotland Island. The Gotland link was followed by many undersea HVDC links in the Baltic Sea. Figure 2.7 shows the undersea HVDC links in the Baltic Sea.

HVDC transmission can also be used to connect systems of different frequency.

Figure 2.7: Undersea HVDC transmission in the Baltic sea.

Figure 2.8 shows the example of the HVDC interconnection between Argentina and Brazil as the frequency in Argentina is 50 Hz and the frequency in Brazil is 60 Hz.

The synchronous connection of very large systems may cause problems that are very difficult to handle such as undamped very low-frequency oscillations. An alternative to such a synchronous connection is an asynchronous one. An example of very large system is the power system of Canada and USA. The east and the west interconnections are connected through HVDC back-to-back links as shown in Figure 2.9.

Another very recent application of HVDC transmission is to overcome AC congested corridors. Building extra AC overhead lines in AC congested corridors might be difficult due to several reasons among the most common is the environmental concern. An alternative is an HVDC link with underground cables. A very good example of the application is the French-Spain 2000 MW HVDC link.

Figure 2.8: Connection of systems of different frequency.

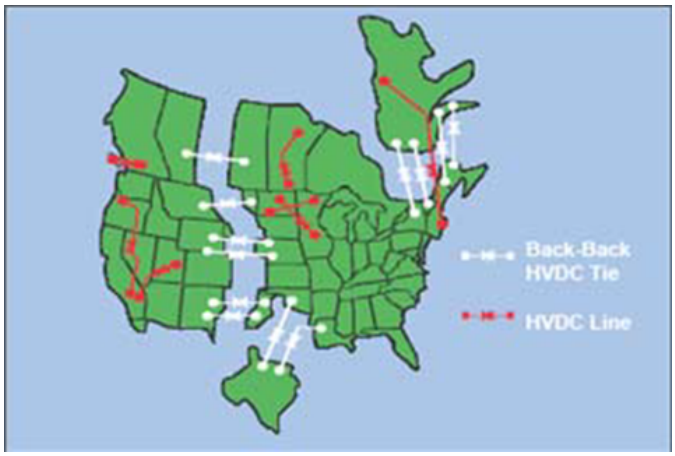

Figure 2.9: Asynchronous connection of very large systems.

2.2 LCC versus VSC technologies

Two HVDC technologies can be found: HVDC based on Line Commutated Converters (that make use thyristor switches) or HVDC-LCC and HVDC based on Voltage Source Converters or HVDC-VSC (that make use of IGBT switches).

HVDC-LCC technology makes use thyristor switches. Twelve-pulse bridge configuration is typically used. It determines the need for harmonic filters. Thyristor bridges always consume reactive power which is provided by the harmonic filters and extra reactive power compensation equipment. Thyristor valve commutation can only occur if the grid impedance is low (high grid short circuit capacity). Hence, synchronous compensators must be added in case of high grid impedance. An alternative to synchronous compensator addition is series compensation of the grid impedance.

HVDC-VSC makes use of IGBT switches. Pulse width modulation of voltages combined with filters is used to produce sinusoidal currents with very low harmonic content. Hence, specific harmonic filters are not needed. VSCs can either produce or consume reactive power independently of active power flow. VSCs can work with high grid impedances (low grid short circuit capacity) at the connection point as their controls are tuned for such conditions.

Table 2.2 summarises the key comparisons between LCC and VSC.

	HVDC LCC	HVDC VSC
Types of switches	Thyristor, line commutated	IGBT, self commutated
Change of power direction	Change of DC voltage	Change of current direction
Reactive power	The reactive power consumed by a LCC converter is 50-60% of active transmitted power	Active power can be controlled independent of the active transmitted power
Minimum power	3% of power rating	No minimum
Converter losses (each one)	~ 0.8%	~ 1.6%
Station space L × W × H of a 600 MW onshore station	200m ×120m ×22m	120m ×50m ×11m
Telecommunication	Needed for start and operation	Not needed (may be needed in multiterminal operation)
Multiterminal operation	Complex to build an d operate, in reality limited to three terminals	Can be built easily
Auxiliary power generator required at offshore platform	Yes	No
Control	Phase angle control 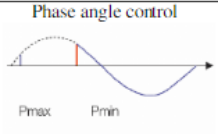	Pulse width controls both active and reactive power 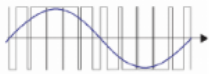
PQ-plane operation	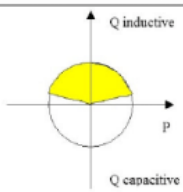	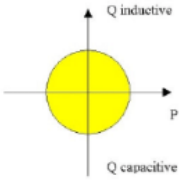

Table 2.2: LCC vs VSC characteristics summary [7]

2.3 Multi-terminal HVDC systems

As mentioned, prior to the physical implementation of these Multi-Terminal HVDC-VSC grids, a simulation tool has to be developed. So this work is industrially desirable to the extent to which these physical grids are desirable. This section will discuss Multi-Terminal grids.

Having discussed the advantages of HVDC in section 2.1, we must now examine if creating a grid out of these point-to-point (P2P) HVDC transmissions is something worth wile doing.

Firstly, multiple P2P links will more likely cause redundancies. A grid like structure will increase the security of power supply and robustness of the grid as a whole. Multi-Terminal systems will reduce costs and reduce losses when compared to P2P links. Additionally, such grid like style will reduce the visual impact when compared to AC (lesser rights of way) and when compared with several single HVDC links.

Without undermining these points, we can also analyse the current state of a more developed electrical distribution technology, AC. AC is said to be the largest machine humanity has ever created. The extent to which it's been interconnected and gridded would be unimaginable at its start. Therefore, it could be bold to state that HVDC wouldn't follow a similar path, to a lesser extent as its use is justified for different purposes.

The following table 2.3, shows a comparison between the current state and the future state of HVDC links according to ABB - Hitachi. It shows that the tendency is fore the P2P links to convert into Multi-Terminal, more versatile grid like systems.

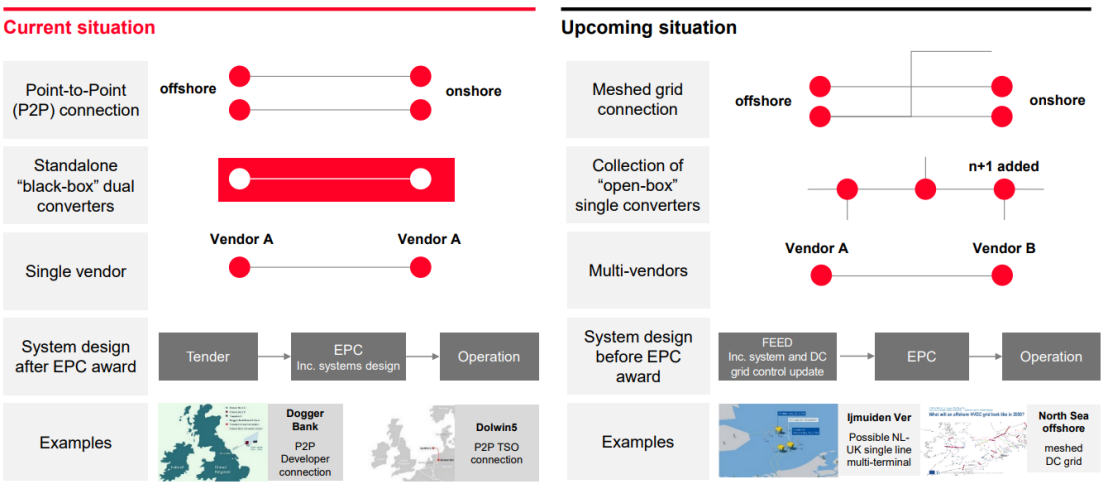

Table 2.3: Comparison of current vs future HVDC systems according to ABB - Hitachi, source: [3]

There are several projects involving the introduction of these grids to the system, some are ongoing and others are being studied. Some of these projects are: the connection of California's offshore wind farms to the AC grid and the Pacific Intertie (studied by IIT), the Atlantic Wind Connection Project, several north sea interconnection projects (such as those studied by the North Sea Energy Cooperation [8]), the studies for The European Supergrid and several other interconnecting grids such as the Sardina - Corsica - Italy interconnection. But, most notably, the first of such connections the Quebec-New England-New York grid.

(a) Atlantic Wind Connection

(b) Pacific Intertie

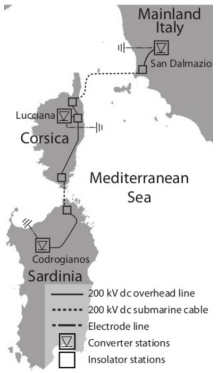

(c) SACOI interconnection

Figure 2.10: Example HVDC projects around the world [9]

The increased amount of renewable sources and the benefits of such grids for certain applications related to these sources, translates into a rise in the number of VSC - HVDC connections, as mentioned in the Hitachi ABB report 'Global Rise of HVDC and Its Background' [10]. This is followed by a desire on the interconnection of such links to create Multi-Terminal HVDC grids. The main reasons being: the strengthening of the electric grid, increased efficiency for bulk transmissions when integrating renewable sources (specially from remote locations), increase the security of supply and allow for a higher utilization of infrastructure [3].

As a brief conclusion, HVDC has reached a level of maturity that could enable larger scale Multi-Terminal HVDC systems. This would help with the energy related problems by increasing the renewable capabilities by interconnecting remote sources, larger consumption regions, scaling up offshore wind industry and increasing international trades. Some possible examples of larger scale Multi-Terminal HVDC systems presented by Hitachi - ABB energy are shown in Figure 2.11.

(a) North Sea interconnection future case scenario

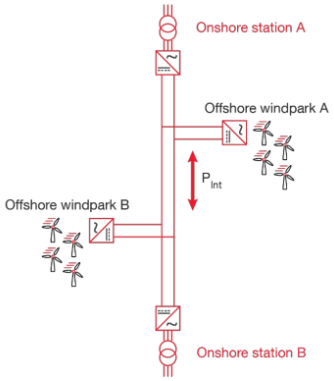

(b) Possible use case for MTDC HVDC for offshore applications

(c) Graphical representation of a European Supergrid

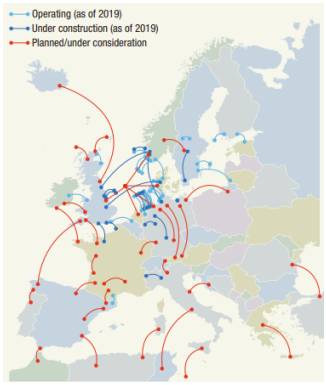

(d) Construction of VSC HVDC in Europe

Figure 2.11: Current and possible future uses of VSC - HVDC multi-terminal interconnections [3]

2.4 Milestones in the development HVDC transmission

This section will act as a summary of the key events during the development of HVDC transmissions, by using some of the most known cases and discussing their implications [4]. Starting with the early stages, technical breakthroughs required [11] and demonstrations of the advantages of such links on real world examples [10].

Figure 2.12: Images of the Gotland Project [12]

Early Concepts and Pioneering Efforts(1870s-1960s):

1881 Thomas Edison's work on direct current (DC) power systems provides a foundational understanding for early electrical transmission. It is in this year where the first power system is built around the Pearl Street Station.

1929 Uno Lamm, a Swedish engineer, contributes to the pioneering efforts in HVDC technology which will result in the first subsea HVDC link in 1954. He was referred to as 'The Father of HVDC'. During his career he obtained 150 patents and worked on projects such as the mercury arc valve, Sweeden's first nuclear reactor and the Pacific Intertie amongst others.

1954 The Gotland project in Sweden becomes the world's first commercial HVDC link, connecting Gotland Island to the Swedish mainland. 20MW / 200A / 100kV line built by ASEA.

1957 Invention of the **Thyristor** valve. Improving the predictability and significantly reducing maintenance.

1961 First HVDC Cross-Channel link is built by ASEA, 160MW. Due to fishing nets and other complications the downtime of the link is large.

1965 The Pacific DC Intertie in the United States, linking the Pacific Northwest and Southern California, demonstrates the feasibility of long-distance HVDC transmission. Largest one built at the time and the last one mercury arc valve project. 1440 MW / 400kV.

1967 One of the mercury-arc valves from the Gotland Link is replaced by a Thyristor valve.

Commercialization of HVDC (1970s-1980s):

1972 Nelson River Bipole I and II projects in Canada connect remote northern hydroelectric plants to the main population centers to the south, showcasing the commercial viability of HVDC. They were the first projects to use water-cooled HVDC valves.

1982 The Sardinia-Italian mainland HVDC link integrates the island of Sardinia with the Italian grid, improving grid reliability. In 1988 a third converter will be installed in Corsica, instituting the first Multi-Terminal HVDC link to ever be completed, SACOI grid.

1984-1987 The Itaipu HVDC link proves the utility of asynchronous connection of different frequency grids as well as bulk power transmission. It is one of the longest and most powerful HVDC lines, connects the Itaipu hydroelectric plant in Paraguay (50Hz) to the Brazilian city of São Paulo (60Hz). The Itaipu power rating was the highest ever seen in HVDC – two bipoles at 6,300 MW / 600 kV. Figure 2.13.

1986 The Cross-Channel HVDC line connects the power grids of France and the United Kingdom, facilitating cross-border energy exchange. 2000MW.

1986 The high earthquake-proofing of suspending the valves in the Intermountain Power Project in the U.S., sets a new standard.

(a) Itaipu HVDC link on a map

(b) Itaipu hydroelectric power station

Figure 2.13: Itaipu Project [4]

Advancement and Integration Era (1990s-2000s):

1992 Quebec - New England link Phase II HVDC project becomes the first large-scale Multi-Terminal HVDC transmission contracted in the world. Figure 2.14

1994 The Baltic Cable, linking the grids of Sweden and Germany, highlights the growing importance of cross-border HVDC integration as it allows for trading and ensuring supply.

1999 First commercial project of **VSC** - HVDC on the Gotland link. Demonstrating the superior dynamic features of this converter, acting as an equivalent synchronous machine with no inertia.

2005 The Basslink project in Australia is the only electrical connection between Tasmania and the mainland grid, the HVDC link enhances energy supply and reliability.

2008 The NorNed project establishes long-distance HVDC connection between Norway and the Netherlands, demonstrating asynchronous connection capabilities. Longest power cable system at 580 km.

2009 The BorWin1 ABB's project in Germany was the first HVDC project for the transmission of power from an offshore wind farm to the mainland grid using VSC HVDC technology. HVDC allowed for a more efficient connection, making the remote link viable and therefore reducing the emissions of CO_2 by 1.5 M Tons/year.

Figure 2.14: Map showing the multi-terminal HVDC-LCC Quebec-New England-New York grid [13]

Current Trends and Future Prospects (2010s-Future):

2012 The ultra-first hybrid HVDC circuit breaker is announced, allowing faster and more precise protection of HVDC systems, lack of which was one of the main impeders of HVDC installation. It interrupts up to 1GW in less than 5ms.

2012 Project Romulo, Spain's first underwater linkage connecting the peninsula with the Baleares islands ensuring the islands electric supply. The connection accounts for around 30% of the island's consumption. The distance, 237 km, and the maximum depth of 1485 m proved to be a daring challenge. But, just in the first year post installation the production of CO_2 produced to power the Baleares islands was decreased by 285 000 Tons [14].

2014 Since the year 2000, 19000 thyristors have been deployed.

2015 The construction of the Spain-France HVDC interconnection is finalised. Its a pioneering link that has an 8 km underground section that traverses the Pyrenees mountains. The 'Pyrenees Electric Highway' was the first project where Siemens used HVDC Plus technology for a link over 1000 MW. Also it's the first time in the world that XLPE insulation is used for these transmission powers.

2017 The Western HVDC Link in the UK connects renewable energy from Scotland to the English grid, highlighting the role of HVDC in offshore wind integration. This project, by Scottish Power, is the highest capacity single sub-sea link in the world.

2020s The DolWin projects in Germany intend on obtaining 65% of its power by renewable energy and so far, has increased its offshore wind production in 6382MW in the last 10 years. All of which use HVDC links, showcasing the utility of such links and increasing the possible advantages of a Multi-Terminal grid.

2020s Ongoing research into advanced HVDC grid structures, like the North Sea Wind Power Hub project, aims to create a large-scale interconnected HVDC grid for offshore wind power.

Future VSC and Hybrid HVDC breakers enables large HVDC Multi-Terminal systems interconnected in a super-grid fashion. Therefore, benefiting from the advantages of long distance, bulk transport and asynchronous connections in its full potential.

Technology	Year first scheme commissioned	Converter Type	Typical Losses per converter (%)[a]	Switching frequency (Hz)[b]	Example Project
HVDC Light 1st Gen	1997	Two-Level	3	1950	Gotland
HVDC Light 2nd Gen	2000	Three-level Diode NPC	2.2	1500	Eagle Pass
	2002	Three-level Active NPC	1.8	1350	Murraylink
HVDC Light 3rd Gen	2006	Two-Level with OPWM	1.4	1150	Estlink
HVDC Plus	2010	MMC	1	<150*	Trans Bay Cable
HVDC MaxSine	2014	MMC	1	<150*	SuperStation
HVDC Light 4th Gen	2015	CTL	1	=>150*	Dolwin 2[c]

*switching frequency is for a single module/cell.

Table 2.4: Table showing the Evolution of VSC-HVDC [15]

(a) North Sea Offshore Wind Farm. Source: Renewable Technology Newsletter.

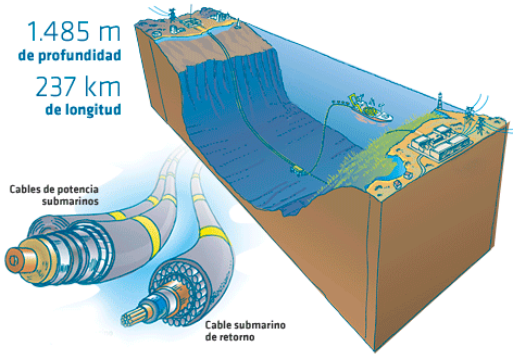

(b) Project Romulo, Peninsula-Baleares interconnection. Source: Red Eléctrica

Figure 2.15: Underwater HVDC projects.

Chapter 3

Steady-state analysis of multi-terminal HVDC-VSC systems with PSS/E

3.1 Introduction

In this chapter the steady-state part of the model will be examined. Firstly the mathematical model for the converters and DC grid is explored with analytical equations, analysing the behaviour and relationship between the HVDC grid, the Voltage Source Converters and the AC grid. The following section will explain how this analysis is then deployed in the PSS/E model. Additionally, this chapter contains the User Guide, alongside required and helpful information for the correct execution of this model. The objective of this model is the steady-state power flow simulation of any user-defined Multi-Terminal HVDC grid with VSC inserted into an AC grid.

3.2 Mathematical Steady-state model [1]

This section describes the steady state mathematical model, alongside a summary of the algorithm used for the previous IIT model. The information has been taken from [1].

The ideas behind VSC modelling for power-flow analysis are depicted in in Fig. 3.1 [16]. Each converter is connected to the AC grid and to the DC grid.

The AC side is modelled by a voltage source $\bar{e}_c = e_c \angle \delta_c$ coupled to the AC bus s ($\bar{u}_s = u_s \angle \delta_s$) through a phase reactor, a capacitor and a transformer ($\bar{z}_c = r_c + j\omega L_c$, $\bar{z}_f = -j1/(\omega C_f)$ and $\bar{z}_{tf} = r_{tf} + j\omega L_{tf}$, respectively). The DC side of the converter is modelled by a current injection i_{dc} into the DC grid. AC and DC sides are related by the energy conservation principle and the converter losses p_{loss} can be calculated using a quadratic function of the converter AC current (rms), i_c, as proposed in [17]:

$$p_c + p_{dc} + p_{loss} = 0, \qquad p_{loss} = a + b \cdot i_c + c \cdot i_c^2, \tag{3.1}$$

The converter is able to control (a) the active power injected into the AC bus, p_s, or the DC voltage, u_{dc}, and (b) the reactive power injected into the AC bus, q_s, or the modulus of the AC voltage, u_s. A general MTDC system with n converters

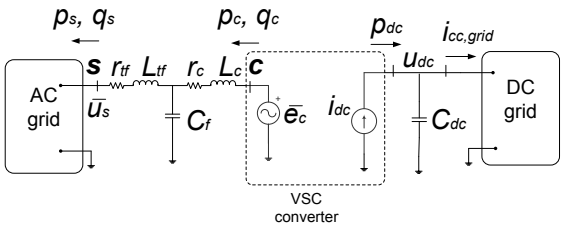

Figure 3.1: VSC converter modelling [16].

and n_L DC lines is considered. For the power-flow analysis, it is assumed that one converter controls the DC voltage (DC slack) and the rest control the active power. The sequential approach proposed in [18] has been used because it can be easily implemented in tools such as PSS/E without modifying the AC power-flow algorithm. Therefore the use of MTDC technology can be easily explored using existing cases of large AC systems. The algorithm runs as follows:

1. The k-th external iteration starts with an initial guess of the active power injected into the AC grid by the VSC at the DC-slack bus ($p_{s,n_s}^{(k)}$, n_s is the index of the DC-slack bus). If available, the results for iteration $k-1$ are used.

2. An AC power flow is calculated (calling PSS/E) taking the variables of the current external iteration k as the initial state (or an initial guess, if started from scratch). All the converters are PQ or PV buses (at the s-bus in Fig. 3.1), depending whether they are controlling the reactive power or the AC voltage. The specified active power of the non-slack converters is constant during the external iteration whilst the specified active power of the DC-slack is allowed to vary during the external iteration ($p_{s,n_s}^{(k)}$). This is a traditional AC load flow with its own slack bus.

3. The AC/DC coupling for each converter is solved. The connection impedance is taken into account to calculate $p_{c,i}^{(k)}$ (at c-bus in Fig. 3.1) from the s-bus data. The converter losses are also calculated to obtain the power, in the DC side of each converter station, for the inner DC power flow ($p_{dc,i}^{(k)}$).

4. The DC power flow (using a Newton-Raphson algorithm) is solved. The DC-slack bus specifies the fixed DC voltage (u_{dc,n_s}^{0}) and the rest of DC buses specify the active-power injection ($p_{dc,i}^{(k)}$, which are data for the DC power flow, but are updated as described in the previous point). DC voltages are obtained together with the power of the DC slack ($p_{dc,n_s}^{(k)}$).

5. DC-slack iteration (ℓ): A new value of $p_{s,n_s}^{(k+1)}$ is obtained, iteratively, from $p_{dc,n_s}^{(k)}$ taking into account the converter losses [18]:

   (a) Initial value: $p_{c,n_s}^{(\ell=0)} = p_{c,n_s}^{(k)}$.

   (b) Solve the branch $s, n_s - c, n_s$ (Fig. 3.1, for the DC-slack bus n_s) with the data: u_{s,n_s}, δ_{s,n_s}, q_{s,n_s} and $p_{c,n_s}^{(\ell)}$ (Newton-Raphson method).

   (c) Obtain the new value of $p_{c,n_s}^{(\ell+1)}$ with p_{dc,n_s} and $p_{loss,n_s}(i_{c,n_s}^{(\ell)})$ using (3.1).

   (d) If $|p_{c,n_s}^{(\ell+1)} - p_{c,n_s}^{(\ell)}| < \epsilon$, stop; if not, put $\ell = \ell + 1$ and return to step b). The output is $p_{s,n_s}^{(k+1)}$.

6. Convergence test: If $|p_{s,n_s}^{(k+1)} - p_{s,n_s}^{(k)}| < \epsilon$: stop and if not, put $k = k + 1$ and return to step 1).

The main subroutine was programmed in Python and calls PSS/E at each external iteration to solve the AC power flow. The DC power flow and the DC-slack iteration are also coded in Python. The final solution of the power flow can later be used by PSS/E as the initial operating point for dynamic simulation.

3.3 PSS/E model

This section will now discuss the simulation model in more depth. This section will be treated as a software documentation for the correct use of this PSS/E tool. This section is organised in the following manner. The tool is defined alongside its objectives, continued by the requirements and model limitations. Then, the processes needed for the installation and modification of the tool are explained. The next subsection acts as the User Guide for the steady-state model. The closing

subsections will comment on the system architecture, data management and model outputs including some key model messages during execution.

3.3.1 Definition of the model

Functionality

The software developed seeks to simulate the power flow on one or several, user-defined, HVDC grids introduced in an existing AC grid. This software appears due to the need of simulating and studying the effect of introducing HVDC – MTDC grids with VSC into an AC grid prior to physical implementation. The first concern of any of such studies is the steady-state analysis, as it the main operational mode. The lack of such simulations on widely used power flow programs, such as PSS/E, was the main cause for the development of this software.

Objectives

The objective is to simulate the power flow of the entire grid when introducing these, user defined, HVDC – MTDC grids. Whilst maintaining the generalizability required by the user to introduce any HVDC grid with its characteristics. The final outcome should be a power flow report of the HVDC grid and the converters. Also, there should be an executable PSS/E AC grid to get obtain the steady state report with the HVDC grid and converters simulated as equivalent generators.

Users

For this section of the model there is no real computer knowledge requirement for the user. Some knowledge of python is helpful for the introduction of the DC data. As mentioned above this power flow simulation is the first step in understanding how a grid works, so the user would be any researcher or company looking for the better analysis of the impact of these grids into an AC grid.

3.3.2 Requirements

General Requirements

These requirements are a brief listing of the steps the program needs to take to achieve a successful steady-state simulation. The explanation will begin assuming the user has stated all the required data following the User Guide and the main python file is executed.

Firstly, the main python file will gather the data from the different user defined HVDC grids and converters saved in functions on a separate python file. Then, PSS/E is initiated, and the main power flow convergence loop is started. There the DC grid power flow is calculated. This result is now introduced into the AC grid in PSS/E as new generators, applied at the AC nodes where the DC grid is linked to the grid by converters. These generators have a steady state equivalence with the defined HVDC grid. PSS/E is then deployed to converge the new AC grid. These two steps are repeated until convergence. The criterion for this convergence is determined by reaching a maximum tolerable difference between the DC grid and the AC grid steady-states.

Functional Requirements

These requirements involve the software requirements that the system has to provide for the correct evolution of the simulation. Most of these requirements are external to the simulation tool (such as PSS/E and Python), others are a list of the required files to be placed in the same folder as the main simulation tool.

As mentioned, there are some system functional requirements, the external requirements are the following ones. A version of PSS/E is required, the student version is valid but will tolerate only smaller grids. PSS/E 34.7.0 was used when developing this program, any newer versions will be valid. A python version tolerated by PSS/E is required. For the mentioned PSS/E the required version is 2.7 (32 bit), it is recommended to use the python GUI that is automatically installed with PSS/E, called IDLE, for an easier linkage of these two programs. The Python libraries imported for the simulation are sys, os and numpy. These have to by accessible by the python version being used at the time of execution.

For the steady-state power flow simulation the following is the list of files required for the correct execution of the program:

AC grid A prior AC grid in PSS/E saved as a '.SAV'. It is in this grid where the HVDC will be introduced.

main The main python file where the execution takes place. This file will then go on and call the reminding python files.

define_grids_mtdc File which contains the data about the structure of the HVDC grid, the parameters of the DC lines and the parameters of the VS Converters.

funs_ACDC File which stores the python functions used for the steady-state calculations. It is here where most of the analytical equations are contained.

run_ACDC File that performs the main convergence loop, creates the final PSS/E files and outputs the data both as a report on screen and as .txt files, these files' names are preceded by the word data.

Legacy

The multi grid VSC-HVDC Multi-Terminal simulation tool here explained was based of the simulation program and mathematical models developed by Dr. Francisco Javier Renedo Anglada at Instituto de Investigación Tecnológica (IIT) in 2013. These calculations allow for an accurate simulation, the validity of such has been proven in the article: 'Development of a PSS/E tool for power-flow calculation and dynamic simulation of VSC-HVDC multi-terminal systems' [1].

Model Limitations

The next paragraph explains some limitations to the simulation model, that limit its use or some situations that will prevent the correct execution of the model.

As any power flow tool, convergence for any case is not granted. Care must be taken when deciding the grid studied and its parameters or convergence may not be achieved. The converter identifier used when importing the model generators into the AC PSS/E grid is '14'. Meaning there must be no other generators with this identifier in the same nodes or in the AC grid. It is assumed that the DC nodes are numbered in an orderly ascending manner starting at 1 and using a non-repeating sequence. It is also assumed that the Power base unit (p.u) is the same for every HVDC grid included, if different values are stated, the base value for the first grid is used. There are some limitations linked the the PSS/E version employed. For example the student version will have a lower limit on the maximum number of nodes and generators.

3.3.3 Procedure

This subsection deals with the procedure needed when performing certain tasks with the code of the model. This section does not act as a User Guide of the whole model, it is more a selection of areas where care mus be taken when tweaking the original code for aspects like modification and installation.

In Installation

Firstly all the files must be included into the same folder. Once there, there is a number of modifications to be made to link the python files to PSS/E.

The path of installation of PSS/E where the python files **psse34** and **psspy** are located has to be pasted into the variable named pssepath in line 45 of the main python file. Usually it will have a similar path to: *"C:\Program Files (x86)\PTI\PSSE34\PSSPY27"*, observe that as we are using Python version 2.7 we access the folder PSSPY27.

In the case that we are using the student version, the file **psse34** will be called **pssexplore34**. Therefore, note that if the student version is used, the line 65 of the python file 'run_ACDC' must be modified, change import psse34 to import pssexplore34.

Currently it is set up to link with PSS/E 34, with a python version 2.7.

3.3.4 User Guide

This subsection is dedicated to the User Guide of the steady-state model for the simulation of HVDC-VSC multi-terminal grids. It will first explain the necessary adaptations of the code required for the execution. Assuming a correct installation, meaning the PSS/E and Python are linked correctly as explained in the above paragraph and all the required files stated in 3.3.2 are included in the same directory. Then, the variables used in the mathematical calculations that are extracted from the user defined grids and converters are explained.

All python files have a brief comment section in the first few lines explaining the key information of each file. It will, nevertheless, be explained in more depth in the section on system architecture 3.3.5.

Execution

Before the first execution ensure that the requirements explained in 3.3.2 are covered. Also, ensure that the link between Python and PSS/E has been successful.

For the steady-state simulation only 2 Python files need to be opened: the main file and the DC grid definition file 'define_grids_mtdc'.

The modifications of the Python files to be made prior to its execution are:

1. In line 39 of the main file, paste the path to the folder where the PSS/E .SAV file containing the AC grid is located. The variable that stores this path is called: strpath.
2. In line 45 of the main file, paste the path to the folder where PSS/E is installed, following the guidance given in the installation steps.
3. In line 50 of the main file, add as many MTDC grids as you need for your simulation following the given structure:

   $$redesDC.append(define\_grids\_mtdc.MTDC\_i())$$

   These will come in the form of Python functions stated in the 'define_grids_mtdc' file and then imported to the main Python file.
4. Modify the file 'define_grids_mtdc' defining as many HVDC-VSC multi-terminal grids as desired with the parameters required for the DC buses, lines and converters. The parameters included in this definition are explained in the next section.

Variables and Parameters

The definition of each of the HVDC-VSC grids has several parameters needed for the steady-state calculations. Each DC grid's data is stored as a Python Dictionary, organised into 4 categories: baseMVA, converter, dcbus and dcbranch.

The first one has only one value stored, the base value for the power in MVA.

The second one has data stored on the converters and the AC/DC coupling. It is stored as an array, each line provides information about a single converter on a specific bus. The parameters that need to be included in this definition are:

- DC bus number
- AC bus number
- rt
- xt
- bf
- rc
- xc
- a
- b
- crect
- cinv
- Pmax
- Pmin
- Qmax
- Qmin
- rateA
- rateB
- rateC
- ratio
- angle
- status
- angmin
- angmax

The third one has data stored on the DC buses. It is stored as an array, each line provides information about a single DC bus. The parameters that need to be included in this definition are:

- DC bus number
- type1: 1: node P, 2: dc-slack
- type2: 1: control of Qs, 2: control of u_s
- Us
- delta_s
- Ps
- Qs
- Udc
- Pdc_iny
- Idc
- Gdc
- Cdc
- Area
- baseKV
- zone
- Vmax
- Vmin

The last one has data stored on the DC branches. It is stored as an array, each line provides information about a DC branch. The parameters that need to be included in this definition are:

- from DC bus number
- to DC bus number
- r
- Ldc
- Ccc
- rateA
- rateB
- rateC
- ratio
- angle
- status

Once these changes are made and the features are set to the specific parameters for the required simulation, the main python file can be executed.

3.3.5 System Architecture

Hierarchy

The steady-state program is made up of the 4 python codes mentioned in the functional requirements 3.3.2. The main file calls the define file to import the HVDC-VSC grid data. Then, the main convergence loop is started.

Module Descriptions

main The main python file, its where the execution takes place. First the necessary functions for the hybrid sequential ACDC power flow are imported. Followed by the import of the definition of MTDC grids. Next the paths for the folder where the AC PSS/E .SAV file is saved and the path for the PSS/E are taken care of. Finally, the HVDC-VSC data from the multiple grids is appended and the run_ACDC function is called.

define_grids_mtdc File which contains the data about the structure of the HVDC grid, the parameters of the DC lines and the parameters of the VS Converters as mentioned in 3.3.4.

funs_ACDC File which stores the python functions used for the steady-state calculations. It is here where most of the analytical equations are contained. The list of functions and their use is:

FJacobian_DC: Function that builds the Jacobian matrix of a DC grid.

makeYdcbus: Function that build the bus admittance matrix of a DC grid Ydc.

incidenceDCmatrix: Function that build the incidence matrix of the DC grid.
The matrix is given by:
Ac(i,j) = +1 if i and j are connected and the line is Lij
Ac(i,j) = -1 if i and j are connected and the line is Lji
Ac(i,j) = 0 if i and j are not connected

powerflow_DC: This function obtains the power flows of a DC grid. The initial values are: Udc_0: Voltages (p.u) (all buses) Pdc_0: Injected powers (p.u) (all buses) Ydc: Ybus of the DC grid (p.u) it is assumed that the dc-slack bus is the last node

runpf_DC: This function solves the power flow equations of a DC grid. The input (ppc) is a file in PYPOWER format, including the data of the dc grid.

slack_it_DC: This function calculates the dclack iteration: main idea: obtain p_s such that is compatible with pdc

run_ACDC File that performs the main convergence loop, the steady-state equations are solved here. The calculations are a sequential AC/DC Power Flow algorithm for multi-terminal VSC-HVDC systems using python and PSS/E. PSS/E solves the AC grid and python solves the DC grid and the coupling between both grids. All the converters are modeled as equivalent generators in PSS/E. It also creates the final PSS/E files and outputs the data both as a report on screen and as .txt files, these files' names are preceded by the word data. These .txt files will then be used in the dynamic simulation.

3.3.6 Model Output

The steady state simulation will print some statements at every iteration to ensure the correct convergence of such loop. It will also provide the PSS/E convergence report and the final HVDC grid data in a table format. Also, a message will appear informing on the reason for exiting the convergence loop. On the folder 8 text result files will appear, these are:

1. The incidence matrix
2. The bus numbers of the DC grid and their number in the AC grid.
3. Cdc data
4. Gdc data
5. Ldc data
6. Rsdc data
7. The initial voltage of the DC buses in p.u.
8. The admittance matrix, Ydc.

Alongside the text files a PSS/E .SAV file with the added DC grid (simulated as generators of id '14') will appear.

Chapter 4

Dynamic analysis of multi-terminal HVDC-VSC systems with PSS/E

4.1 Introduction

In this chapter the dynamic state part of the model will be examined. Firstly the mathematical model is explored with analytical equations. The equations determined in this section analyse the behaviour of the HVDC grid and that of the VSC in relationship with the AC grid. The following section will explain how this analysis is then deployed in the PSS/E model. Additionally this chapter contains the User Guide alongside required and helpful information for the correct execution of this model for the dynamic simulation of any user defined multi-terminal HVDC VSC grids inserted into an AC grid.

4.2 Mathematical dynamic model [1]

This section describes the dynamic mathematical model, alongside a summary of the algorithm used for the previous IIT model. The information has been taken from [1].

The dynamic model for MTDC systems to be used in PSS/E was intended for electromechanical dynamic simulation, which covers time constants from 0.01 s to 10 s [19]. Electromechanical models of a power system take into account the slow dynamics of synchronous machines, their controllers and other devices, whilst the

AC branches are assumed to be quasi-static. The model was split into converter models and the DC-grid model.

4.2.1 VSC station model

Regarding the VSC model shown in Fig. 3.1: the AC side of the converter and the rest of the AC grid were assumed to be quasi-static whilst the VSC is controlled using vector control where the AC voltage is aligned with the d-axis: $\bar{u}_s = u_s + j0$. Therefore, the active and reactive-power injections of the VSC are $p_s = u_s i_{s,d}$ and $q_s = -u_s i_{s,q}$.

Active and reactive power are controlled with an inner current loop and with an outer controller [16]. The inner loop time constants (1-10 ms [20]) are much faster than the ones of the synchronous generators and their controllers and they have been approximated by a first order system, as shown in Fig. 4.1, where $i_{s,d}^{ref}, i_{s,q}^{ref}$ are the current references. Either the active power p_s or the DC voltage u_{dc} is controlled with the d-axis current $i_{s,d}$ using PI controllers, as depicted in Figure 4.1a. Similarly, the q-axis current is used to control either the reactive power or the AC-voltage modulus (Fig. 4.1b). The time constants of the outer loops are between 1ms and 100ms [20].

The converter model was implemented with the operating limits for active and reactive power: P_{max}, P_{min}, Q_{max}, Q_{min} and with the maximum current limit $i_{s,max}$, which can be set to d-axis priority, q-axis priority or equal priority [21]. The maximum output AC voltage of a VSC depends on the DC voltage and the maximum modulation index ($e_{c,max} = m_{max} u_{dc}$) [22] and this limit is also taken into account: if $e_c^{ref} > e_{c,max}$, the current references are re-calculated using $e_{c,max} \angle \delta_c^{ref}$ as internal voltage, as depicted in Fig. 4.1.

4.2.2 DC-grid model

The dynamic model of the DC grid includes the converters, the capacitors and the cables, as in [16]. The inputs of the system are the current injections, $\boldsymbol{I_{dc}} = (i_{dc,i}) \in \mathbb{R}^{n \times 1}$, which model the converters. DC cables are represented by an equivalent π-model, with resistance $r_{dc,ij}$, inductance $L_{dc,ij}$ and capacitance $C_{cc,ij}$ (Fig. 4.3). An equivalent capacitor at each DC bus is used to model the capacitor of the converter, $C_{VSC,i}$, and the capacitance of the DC lines ($C_{dc,i} = C_{VSC,i} + \sum_{j \neq i} C_{cc,ij}/2$).

The model also includes a shunt conductance $g_{dc,i}$ at every DC bus that can be used to model resistive loads. The state variables of the system are the DC

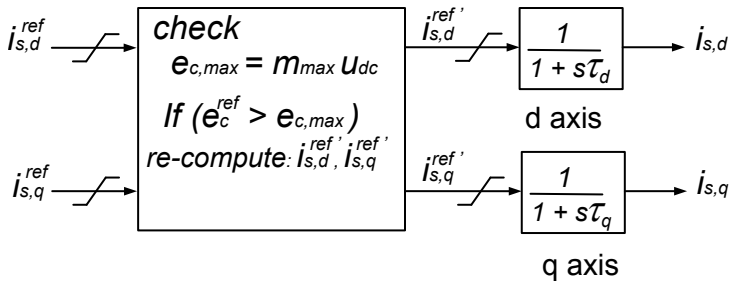

Figure 4.1: Approximation of the inner current loop.

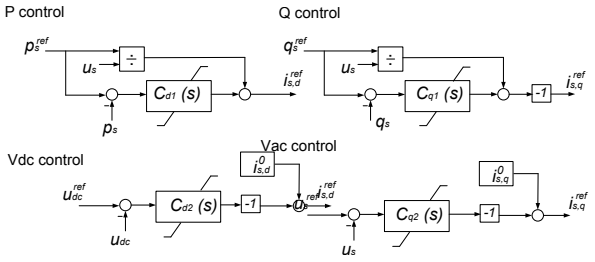

(a) d-axis. (b) q-axis.

$C_x(s) = K_{p,x} + K_{i,x}/s$ where x can be $d1$, $d2$, $q1$ or $q2$

Figure 4.2: Outer controllers.

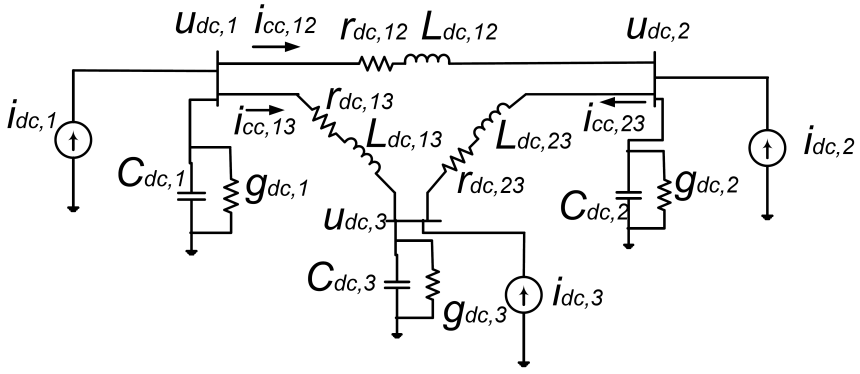

Figure 4.3: Dynamic model of the DC grid.

voltages, $\boldsymbol{U_{dc}} = (u_{dc,i}) \in \mathbb{R}^{n\times 1}$, and the currents through the DC lines, $\boldsymbol{I_{cc}} = (i_{cc,\ell}) \in \mathbb{R}^{n_L\times 1}$. Therefore, the differential equations for the DC grid are [16]:

$$\boldsymbol{C_{dc}}\frac{d\boldsymbol{U_{dc}}}{dt} = -\boldsymbol{G_{dc}}\boldsymbol{U_{dc}} - \boldsymbol{A_c}\boldsymbol{I_{cc}} + \boldsymbol{I_{dc}} \tag{4.1}$$

$$\boldsymbol{L_{dc}}\frac{d\boldsymbol{I_{cc}}}{dt} = \boldsymbol{A_c^T}\boldsymbol{U_{dc}} - \boldsymbol{R_{dc}}\boldsymbol{I_{cc}} \tag{4.2}$$

$$\text{where:} \quad \boldsymbol{G_{dc}} = \text{diag}(g_{dc,i}),\ \boldsymbol{C_{dc}} = \text{diag}(C_{dc,i}) \in \mathbb{R}^{n\times n} \tag{4.3}$$

$$\boldsymbol{R_{dc}} = \text{diag}(r_{dc,\ell}),\ \boldsymbol{L_{dc}} = \text{diag}(L_{dc,\ell}) \in \mathbb{R}^{n_L\times n_L} \tag{4.4}$$

and $\boldsymbol{A_c} = (a_{i\ell}) \in \mathbb{R}^{n\times n_L}$ is the incidence matrix of the DC grid, whose elements are:

$$a_{i\ell} = \begin{cases} +1 & \text{if line } \ell \text{ is defined leaving node } i. \\ -1 & \text{if line } \ell \text{ is defined entering node } i. \\ 0 & \text{if line } \ell \text{ is not connected to node } i. \end{cases} \tag{4.5}$$

4.2.3 AC/DC coupling

AC and the DC sides of each converter i are coupled by the energy conservation principle (3.1). At each time step, AC and the DC systems are updated sequentially and $p_{dc,i}$ is obtained from $p_{c,i}$. Currents injected into the DC grid are calculated as:

$$i_{dc,i} = \frac{p_{dc,i}}{u_{dc,i}} = \frac{-(p_{c,i} + p_{loss,i})}{u_{dc,i}} \quad \forall i = 1,\ldots,n \tag{4.6}$$

4.2.4 Control of the MTDC system

The most common options for control of MTDC systems are: (a) centralised control, in which one converter controls the DC voltage and the rest control the active power injected into the AC grid and (b) distributed control, in which the DC-voltage control is shared among a set of converters with the so-called DC-voltage droop. In the distributed control scheme, the active-power set point of each VSC is given by [22]:

$$p_{s,i}^{ref}(t) = p_{s,i}^{0} - \frac{1}{k_{dc,i}}(u_{dc,i}^{0} - u_{dc,i}(t)) \tag{4.7}$$

4.3 PSS/E model

This section will now discuss the simulation model in more depth. This section will be treated as a software documentation for the correct use of this PSS \E tool.

This section is organised in the following manner. The tool is defined alongside its objectives, continued by the requirements and model limitations. Then, the processes needed for the installation and modification of the tool are explained. The next subsection acts as the User Guide for the dynamic model. The closing subsections will develop the system architecture, data management and model outputs including some key model messages during execution.

4.3.1 Definition of the model

The MTDC model has been programmed (in FORTRAN) as a PSS/E user-defined model and consists of n "generator-type" models for the converters and one "governor-type" model for the DC grid. DC-voltage droop control or controllers for ancillary services could have been included in the VSC models but, for flexibility, they were implemented in independent models which change the references of the converter models. Along these lines, the DC-voltage control has been implemented as an "exciter-type" model that changes the active-power set point of the converters according to (4.7). Supplementary controllers for transient stability improvement have been included in the simulation tool in very much the same way [23].

Functionality

The functionality of this model is to simulate the dynamic response of the electric grid when one or more multi-terminal HVDC VSC grids are included. Before any implementation of such grids the dynamic response to failures or its response to a change in the operating conditions must be modeled to ensure the grid's resilience. The lack of such simulations on widely used power flow programs, such as PSS/E, was the main cause for the development of this software.

Objectives

As mentioned the main objective is to achieve a reliable tool for the dynamic simulation when any of the dynamic PSS/E events take place. The tool should

produce graphs with this temporary response between steady-states for further analysis. This model should work together with the previous one as the initial state comes form the steady-state calculations. Providing a generalised tool that takes into account the user defined grid in the first model to create the necessary inputs for the dynamic model automatically will minimise human intervention involved in the simulation process, therefore, minimising human error.

Users

Due to the increased complexity of this model certain extra requirements are needed, some of them involve slight FORTRAN coding and compiling. This means that the user needs some knowledge on these topics. Nevertheless, as for the previous steady-state model, the user would be any researcher or company looking for the better analysis of the impact of these grids into an AC grid

4.3.2 Requirements

General Requirements

These requirements are a brief listing of the steps the program needs to take to achieve a successful dynamic simulation. The explanation will begin assuming the user has stated all the required data following the User Guide and the main python file is executed.

First, the steady-state simulation is processed following the steps mentioned in chapter 3. Then, PSS/E is initialised as it will be the main tool used for the dynamic calculations. Next the DYR file containing the necessary dynamic data is created and the steady-state output files are adapted for the correct dynamic lecture. The dll file is imported and the case initialized, this is then followed by the dynamic event and the saving of the data into the output log.

Functional Requirements

These requirements involve the software requirements that the system has to provide for the correct evolution of the simulation. Most of these requirements are external to the simulation tool (such as PSS/E and Python), others are a list of the required files to be placed in the same folder as the main simulation tool.

As the power flow calculations are required prior to the dynamic simulation the requirements for the steady-state, 3.3.2, are also requirements for this section. To avoid repetition, this section will assume those requirements have been fulfilled.

In addition to these, the system requirements for the installation part, as it will be mentioned, a FORTRAN compiler is required to create the DLL file with the correct path. For the dll tool installed with PSS/E there are 2 programs required. An Intel Visual Fortran compiler (IVF), for PSS/E 34 a IVF compiler version 15 is required. To check the version required for your PSS/E, inside the PSS/E tool 'User Model Compile/Link dll', the one employed for the dll creation, there is an information tab wich displays the IVF version needed for each PSS/E version. Also, the visual studio program is required. This programs are only required for the first compilation during installation, once the path has been set up correctly the dynamic model will work without these programs.

For the dynamic simulation the following is the list of files required for the correct execution of the program, remember that the files mentioned in the steady-state model still apply here:

DYR File containing the dynamic data, its created automatically by the python file.

TXT Files containing the result of the power flow calculations, they are created automatically by the python file

FORTRAN files A collection of 8 FORTRAN files that will be compiled into the DLL file. ['DCGRID', 'PDELAY', 'QDELAY', 'SPWDRD', 'SQPODD', SQWDRD', 'SVSCON', 'WDELAY']

MTDC.dll DLL file used by PSS/E for the dynamic simulation of the HVDC-VSC grid via equivalent generators.

funs_Dyn File that contains the main dynamic functions to be used in the main dynamic file.

runDynSim_psseC File that runs the main dynamic simulation, it is called from the runACDCpf_psseJ file in the steady-state calculations.

Legacy

The multi grid VSC-HVDC multi-terminal simulation tool here explained was based of the simulation program and mathematical models developed by Dr. Fran-

cisco Javier Renedo Anglada at Instituto de Investigación Tecnológica (IIT) in 2013. These calculations allow for an accurate simulation, the validity of such has been proven in the article: 'Development of a PSS/E tool for power-flow calculation and dynamic simulation of VSC-HVDC multi-terminal systems' [1].

Model Limitations

The next paragraph explains some limitations to the simulation model, that limit its use or some situations that will prevent the correct execution of the model.

The dynamic model limitations are related to the steady-state model limitations. Additionally, the need for a FORTRAN compiler each time the TXT file path is altered is a big limitation, as it will require a change in the FORTRAN code to account for the new path. Also, the PSS/E student version limitations greatly apply to this section as each equivalent dynamic generator consumes several variables in the PSS/E working memory and the limits of this memory will affect the possible size and number of HVDC grid simulated at once.

4.3.3 Procedure

This subsection deals with the procedure needed when performing certain tasks with the code of the model. This section does not act as a User Guide of the whole model, it is more a selection of areas where care mus be taken when tweaking the original code for aspects like modification and installation.

In Modifications

When modifying any of the FORTRAN files, they must be compiled and the new DLL created so that the changes can be applied by PSS/E.

In Installation

As mentioned above, the use of the dynamic model is dependent on a prior use of the steady-state model. This section will assume the installation for the steady-state model went well and will carry on from there.

The path to the folder where the AC grid is stored as a .SAV file, same path used in the variable strpath of the main python file, has to be copied into: lines 217

to 224 of DCGRID and lines 540 to 541 of SVSCON. Then, using the PSS/E Environment Manager tool to create the DLL files, the FORTRAN files are compiled and the DLL is created. The steps to take for this part are: select the compilation method for your PSS/E version, type the path where the DLL should be created, add MTDC as name of the output file, select the 8 modified FORTRAN files into the User Model Fortran Source Files and select the compile-DLL button.

4.3.4 User Guide

This subsection is dedicated to the User Guide of the dynamic model for the simulation of HVDC-VSC multi-terminal grids. It will first explain the necessary adaptations of the code required for the execution. Assuming a correct installation, meaning the PSS/E and Python are linked correctly as explained in the above paragraph, the FORTRAN modifications have been successful and all the required files stated in 4.3.2 are included in the same directory. Then, the variables used in the mathematical calculations that are extracted from the user defined grids and converters are explained.

All python files have a brief comment section in the first few lines explaining the key information of each file. It will, nevertheless, be explained in more depth in the section on system architecture 4.3.5.

Execution

Before the first execution ensure that the requirements explained in 3.3.2 are covered. Also, ensure that the FORTRAN modification has been successful.

For the dynamic simulation 3 Python files need to be opened: the main file, the DC grid definition file 'define_grids_mtdc' and the dynamic definition file 'funs_Dyn'.

The modifications of the Python files to be made prior to its execution are:

1. In line 48 of the main file, modify the toggle variable with name perform_dyn. True for both a steady-state simulation and a dynamic symulation, False for just a steady-state simulation.
2. Modify the file 'define_grids_mtdc' defining as many HVDC-VSC multi-terminal grids as desired with the parameters required for the DC buses, lines and converters. The parameters included in this definition were explained in the steady-state section 3.3.4.
3. To modify the dynamic data there are 2 different ways:

   Modify all converters equally This can be done by changing the parameter values in the function called Define_Dyr on the python file funs_Dyn. This will make the same modification n all converters of the HVDC grid simultaneously.

   Modify a single converter independently If the intent is to modify only one of the converters it can be done by doing the following. After modifying the steady-state data, allow the simulation to run once freely (with the general dynamic data), that way the template for the DYR will be created. Then, modify the DYR file that has just been produced to include the desired individual parameters. Finally, comment line 46 in python file runDynSim_psseC to avoid the overwriting of the modified DYR and then execute the main python file again. This time it will skip the DYR generation step and will read the newly user modified DYR file.

Variables and Parameters

The definition of each of the HVDC-VSC grids has several parameters needed for the dynamic calculations. The data is stored in a DYR file, this file is used by PSS/E to call the necessary FORTRAN functions using this data as inputs for the dynamic simulation. The structure and parameters used for every FORTRAN file will be listed next.

If there are any technical doubts on how the PSS/E dynamic tool works, how it is linked to this model via the DYR or on the actual structure of the DYR file. It could be helpful to access the chapter 16 of the PSS/E - POM called: Dynamic Simulation Activity Descriptions [24].

DCGRID Governor-type model for the DC grid.

- Structure
  BUSID 'USRMDL' IM 'DCGRID' IC IT NI NC NS NV (data list)
  - BUSID is the AC bus number where the VSC is connected.
  - IM is the id of the equivalent generator, '14'.
  - IC is the turbine model, 5.
  - IT as its not a current injection model, 0.
  - NI is the number of ICONs, 4.
  - NC is the number of CONs, 2.
  - NS is the number of states, $n + nl$. Being n the number of buses in the DC grid and nl the number of lines.
  - NV is the number of VARs, $2 * n$
- Data List
  - n
  - nl
  - number_poles
  - id_grid → grid identifier
  - sum_n → sum of all DC nodes
  - sum_nl → sum of all DC lines
  - curr_n → sum of all DC nodes of HVDC grids prior to the current one, acts as a pointer
  - curr_nl → sum of all DC lines of HVDC grids prior to the current one, acts as a pointer
  - Udc_base_kV → base voltage
  - Pdc_base_MW → base power
  - Udc → dc voltage
  - Icc → converter current
  - Pdc → dc power
  - Idc → dc currents

PDELAY Communication of delays between the terminals of the VSC-HVDC multi-terminal system.

- Structure
  BUSID 'USRMDL' IM 'PDELAY' IC IT NI NC NS NV (data list)
  - BUSID is the AC bus number where the VSC is connected.
  - IM is the id of the equivalent generator, '14'.

- IC is the stabilizer model, 3.
- IT as its not a current injection model, 0.
- NI is the number of ICONs, $n_vsc + 2$. Being n_vsc the number of Voltage Source Converters.
- NC is the number of CONs, $n_vsc + 1$.
- NS is the number of states, $2 * n_vsc$.
- NV is the number of VARs, $n_vsc + 2$

- Data List

  · m_onoff → enable/disable the delays
  · Tau → delays
  · n_vsc → number of converters
  · OMEGA_ms → frequency references
  · sigma
  · x → state variables
  · I_BUSES → bus number
  · d_x → dstate variables

QDELAY Synthetic Inertia - Reference calculation, Communication of delays between the terminals of the VSC-HVDC multi-terminal system

- Structure
  BUSID 'USRMDL' IM 'QDELAY' IC IT NI NC NS NV (data list)
  - BUSID is the AC bus number where the VSC is connected.
  - IM is the id of the equivalent generator, '14'.
  - IC is the stabilizer model, 3.
  - IT as its not a current injection model, 0.
  - NI is the number of ICONs, $n_vsc + 2$. Being n_vsc the number of Voltage Source Converters.
  - NC is the number of CONs, $n_vsc + 1$.
  - NS is the number of states, $2 * n_vsc$.
  - NV is the number of VARs, $n_vsc + 2$

- Data List

- m_onoff → enable/disable the delays
- n_vsc → number of converters
- sigma
- I_BUSES → bus number
- Tau → delays
- OMEGA_ms → frequency references
- x → state variables
- d_x → dstate variables

SPWDRD

- Structure
  BUSID 'USRMDL' IM 'SPWDRD' IC IT NI NC NS NV (data list)
  - BUSID is the AC bus number where the VSC is connected.
  - IM is the id of the equivalent generator, '14'.
  - IC is the exciter model, 4.
  - IT as its not a current injection model, 0.
  - NI is the number of ICONs, 3.
  - NC is the number of CONs, 13.
  - NS is the number of states, 3.
  - NV is the number of VARs, 14.
- Data List
  - delta_dc → enable dc-voltage droop
  - delta_freq → enable freq-droop: 1: ENABLE, 2: erik, 3:disabled
  - delta_a → enable synthetic intertia
  - Tf → freq filter time constant [s]
  - Tw → Washout filter time constant [s]
  - Kdc_nom → DC-voltage droop gain
  - Kp_nom → proportional gain (p.u-nom)
  - K_alpha_nom → synthetic inertia gain
  - udc_thres → freq-deviation threshold to enable freq-droop [p.u]
  - w_thres → freq-deviation threshold to enable freq-droop

[p.u]

- alpha_thres → freq-derivative threshold to enable freq-droop [p.u/s]
- bbps_max_nom → Pmax (p.u-nom)
- bbps_min_nom → Pmin (p.u-nom)
- d_Pmax_nom → maximum active power derivative (p.u/s)
- bbps_erik_nom → maximum active power derivative (p.u/s)
- ps_ini → Reference active power, coincides with load flow values.
- w_ini
- w_bus
- ps_ref
- bbps_ref
- d_ps_ref_supp
- udc_ini
- udc
- m_dc
- bbps_ref_dc
- bbps_ref_freq
- bbps_ref_H
- desv_w_ini
- uw
- omega_est_i
- w_fil → filtered frequency
- w_ini_fil → filtered frequency
- xw → state of the washout filter
- d_w_fil → derivative of filtered frequency
- d_w_ini_fil → derivative of filtered frequency
- d_xw → dstate of the washout filter

SQPODD Synthetic Inertia - Reference calculation, Communication of delays between the terminals of the VSC-HVDC multi-terminal system

- Structure
  BUSID 'USRMDL' IM 'SQPODD' IC IT NI NC NS NV (data list)
  - BUSID is the AC bus number where the VSC is connected.
  - IM is the id of the equivalent generator, '14'.
  - IC is the stabilizer model, 3.
  - IT as its not a current injection model, 0.

- NI is the number of ICONs, 3.
- NC is the number of CONs, 16.
- NS is the number of states, 4.
- NV is the number of VARs, 16.

- Data List
  - delta_ac → enable dc-voltage droop
  - delta_freq → enable freq-droop: 1: ENABLE, 2: erik, 3:disabled
  - delta_a → enable synthetic intertia
  - Tf → freq filter time constant [s]
  - Tw → Washout filter time constant [s]
  - Kac_nom → DC-voltage droop gain
  - Kq_p_nom → proportional gain (p.u-nom)
  - K_alpha_nom → synthetic inertia gain
  - us_thres → freq-deviation threshold to enable freq-droop [p.u]
  - w_thres → freq-deviation threshold to enable freq-droop [p.u]
  - alpha_thres → freq-derivative threshold to enable freq-droop [p.u/s]
  - bbqs_max_nom → Qmax (p.u-nom)
  - bbqs_min_nom → Qmin (p.u-nom)
  - d_Qmax_nom → maximum reactive power derivative (p.u/s)
  - bbqs_erik_nom → maximum reactive power derivative (p.u/s)
  - alpha_erik → maximum reactive power derivative (p.u/s)
  - T_s1 → POD: time constant -> numerator
  - a_s1 → POD: parameter for the time constant of the den: $T_{s2} = a_{s1} * T_{s1}$
  - N_s1 → POD: exponent of the lead/lag network
  - qs_ini → Reference reactive power, coincides with load flow values.
  - w_ini
  - w_bus
  - qs_ref
  - bbqs_ref
  - d_qs_ref_supp

- us_ini
- us
- m_ac
- bbqs_ref_ac
- bbqs_ref_freq
- bbqs_ref_H
- desv_w_ini
- uw
- u_pod
- y_pod
- w_fil → filtered frequency
- w_ini_fil → filtered frequency
- xw → state of the washout filter
- x_pod → state of the lead/lag filter
- d_w_fil → derivative of filtered frequency
- d_w_ini_fil → derivative of filtered frequency
- d_xw → dstate of the washout filter
- d_x_pod → dstate of the lead/lag filter

SQWDRD Synthetic Inertia - Reference calculation, Communication of delays between the terminals of the VSC-HVDC multi-terminal system

- Structure
  BUSID 'USRMDL' IM 'SQWDRD' IC IT NI NC NS NV (data list)
  - BUSID is the AC bus number where the VSC is connected.
  - IM is the id of the equivalent generator, '14'.
  - IC is the stabilizer model, 3.
  - IT as its not a current injection model, 0.
  - NI is the number of ICONs, 3.
  - NC is the number of CONs, 13.
  - NS is the number of states, 3.
  - NV is the number of VARs, 14.
- Data List
  - delta_ac → enable dc-voltage droop
  - delta_freq → enable freq-droop: 1: ENABLE, 2: erik,

3:disabled

- delta_a → enable synthetic intertia
- Tf → freq filter time constant [s]
- Tw → Washout filter time constant [s]
- Kac_nom → DC-voltage droop gain
- Kq_p_nom → proportional gain (p.u-nom)
- K_alpha_nom → synthetic inertia gain
- us_thres → freq-deviation threshold to enable freq-droop [p.u]
- w_thres → freq-deviation threshold to enable freq-droop [p.u]
- alpha_thres → freq-derivative threshold to enable freq-droop [p.u/s]
- bbqs_max_nom → Qmax (p.u-nom)
- bbqs_min_nom → Qmin (p.u-nom)
- d_Qmax_nom → maximum reactive power derivative (p.u/s)
- bbqs_erik_nom → maximum reactive power derivative (p.u/s)
- alpha_erik → maximum reactive power derivative (p.u/s)
- V_thres → Q-control strategy is activated only if $V > V_{thres}$
- qs_ini → Reference reactive power, coincides with load flow values.
- w_ini
- w_bus
- qs_ref
- bbqs_ref
- d_qs_ref_supp
- us_ini
- us
- m_ac
- bbqs_ref_ac
- bbqs_ref_freq
- bbqs_ref_H
- desv_w_ini
- uw
- w_fil → filtered frequency
- w_ini_fil → filtered frequency
- xw → state of the washout filter
- d_w_fil → derivative of filtered frequency
- d_w_ini_fil → derivative of filtered frequency
- d_xw → dstate of the washout filter
- d_x_pod → dstate of the lead/lag filter

SVSCON VSC-HVDC Multi-terminal model, VSC converter model, DIFFERENTIAL EQUATIONS SOLUTION

- Structure
  BUSID 'USRMDL' IM 'SVSCON' IC IT NI NC NS NV (data list)
  - BUSID is the AC bus number where the VSC is connected.
  - IM is the id of the equivalent generator, '14'.
  - IC is the generator model, 1.
  - IT as its a current injection model, 1.
  - NI is the number of ICONs, 6.
  - NC is the number of CONs, 24.
  - NS is the number of states, 7.
  - NV is the number of VARs, 33.
- Data List
  - tau → Inverter time constant
  - Kd_p1
  - Kd_i1
  - Kd_p2
  - Kd_i2
  - Kd_d2 → gain of the differential control of Udc; for the DC-voltage control, PID works much better than PI
  - Kq_p1
  - Kq_i1
  - Kq_p2
  - Kq_i2
  - icmax_pu_conv → Maximum inverter current/susceptance in pu with respect to inverter rating
  - Ps_max_MW
  - Ps_min_MW
  - Qs_max_Mvar
  - Qs_min_Mvar
  - udc_max
  - udc_min
  - m_modulation_max
  - A_MW → constant converter loss coefficient (MW): $ploss = a + b * ic + c * ic^2$
  - B_kV → linear converter loss coefficient (kV): $ploss = a + b * ic + c * ic^2$
  - C_rect_ohm → rectifier

quadratic converter loss coefficient (ohm): $ploss = a + b * ic + c * ic^2$

- C_inv_ohm → constant converter loss coefficient (ohm)
- Cdc_uF → capacitor of the converter (micro-Faraday) (uF)
- Udc_nominal_kV → nominal dc-voltage of the converter (kV)
- i_converter → number of the converter
- dcontroltype → Ps-control: 1 , Udc-control: 2
- qcontroltype → Qs-control: 1 , Us-control: 2
- ilimit_prio → Current limit: P-priority: 1, Q-priority: 2 and P-Q equal priority: 3 or any other integer
- n → number of converters in the DC grid
- sum_converters → sum of all DC nodes of HVDC grids prior to the current one, acts as a pointer
- id_grid → identifier of the HVDC grid
- ps_initial → Reference active power, coincides with load flow values.
- qs_initial → Reference reactive power, coincides with load flow values.
- icd_out
- icq_out
- ps
- qs
- icd_ini
- icq_ini
- icd
- icq
- fin_sim
- us_initial
- ps_ref
- udc_ref
- qs_ref
- us_ref
- aux_ilimit
- awu_d
- awu_q
- ic_abs_puconv
- ec_d
- ec_q
- udc
- idc
- idc_ini
- pdc
- delta_s_ini
- udc_ini

· ps_0

· bbps_ref

· qs_0

· bbqs_ref

· m_modulation

· xd → icd

· xq → icq

· md → d-integral state variable type1

· mq → q-integral state variable type1

· ndc → d-integral state variable type2

· nq → q-integral state variable type2

· eta_d → d-integral state variable type3 (passive grid)

· d_xd → icd

· d_xq → icq

· d_md → d-integral state variable type1

· d_mq → q-integral state variable type1

· d_ndc → d-integral state variable type2

· d_nq → q-integral state variable type2

· d_eta_d → d-integral state variable type3 (passive grid)

WDELAY Communication delays between the terminals of the VSC-HVDC multi-terminal system.

- Structure
  BUSID 'USRMDL' IM 'QDELAY' IC IT NI NC NS NV (data list)
  - BUSID is the AC bus number where the VSC is connected.
  - IM is the id of the equivalent generator, '14'.
  - IC is the Branch and 2-winding transformer device model, 9.
  - IT as its not a current injection model, 0.
  - NI is the number of ICONs, $n_{vsc} + 2$. Being n_vsc the number of Voltage Source Converters.
  - NC is the number of CONs, $n_{vsc} + 1$.
  - NS is the number of states, $2 * n_{vsc}$.
  - NV is the number of VARs, $n_{vsc} + 1$
- Data List

- I_BUSES → bus numer of the converters
- Tau → Delays: tau_ki = delay between terminals k and i
- OMEGA_ms → freq references
- x → state variables
- d_x → dstate variables

4.3.5 System Architecture

Hierarchy

The dynamic model consists of the previous 4 steady-state python files plus 2 dynamic python files and 8 FORTRAN files, compiled into a DLL file. First, the steady-state simulation takes place. At the end of this execution the dynamic functions are called, the dynamic model inputs are prepared and the case is initialised with PSS/E. Then, the dynamic event takes place and the PSS/E graphical outputs are produced.

Module Descriptions

runDynSim_psseC Main file that is called after the power flow calculations. As it was mentioned above, the user defined data on the HVDC-VSC grid will be imported to PSS/E via a DYR file, so, after the PSS/E initialization, the first step is to create this file using information from the steady-state user defined grid, the power flow solutions and the dynamic user defined parameters. As the DYR file is complex in structure, the automation helps prevent typing errors. Nevertheless, the modification of this file is explained in 3.

Then the TXT files are adapted so that they can be read by the FORTRAN files. The paths are taken care of and the case is started. A last load flow is performed, the generators are converted to current sources, the loads are converted to constant current and constant admittance loads for P and Q, the converted load file is saved and the user MTDC.DLL model is imported. Then the desired outputs are selected, commented in the python file ther is a list will all possible outputs, with the main ones beeing explained in more detail. The dynamic simulation parameters are introduced and the line parameters are made frequency dependent. Following these steps, the dynamic event is simulated. It is recommended to simulate a short period before the event starts and a longer one after the event has finished to allow

the case to reach steady state. Finally, the output is saved into an .out PSS/E file.

It is recommended to read trough the Dynamic Simulation chapter in the PSS/E - API (pg 1082) [25] for more information on PSS/E specific python codes required when modifying the dynamic simulation and output variables. For information on the output channels pg 1173, and information on PSS/E dynamic disturbances pg 1497.

funs_Dyn File that contains the main functions used in the dynamic model, mainly to organise and create the inputs necessary for the FORTRAN files.

Define_Dyr: Functions that contains the necessary information to be iteratively called to create the DYR for every generator. It is here where any data should be modified to change the dynamic parameter, the changes will apply to all VSC equally.

Generate_gen: Function that creates the gen matrix, this matrix contains information on all the generators of the system to help with the DYR creation. The matrix has the following columns: generator bus number, generator id and a column that indicates if the generator is equivalent to a DC slack converter.

Print_Dyr: Function that generates the final DYR file using the information and functions defined above.

save_data: Function created to simplify the numpy savetext function with the desired characteristics.

Prepare_Fortran: Function that adapts the current TXT files outputted by the steady-state model to a FORTRAN readable format.

4.3.6 Model Output

The dynamic model will print the PSS/E convergence messages and the dynamic PSS/E initialization process messages (ensure that the initial conditions appear OK or with small DSTATE - derivative values, if this is not accomplished then the dynamic simulation output might not be valid). Also, there will be a file produced named output.out, this is a file that contains the dynamic simulation data so that it can be viewed via PSS/E graphical function. To view this output graphs, open the file in PSS/E and access it's content via the Plot Tree tab. Then drag the desired output onto the empty graph on the right of the screen to view it. The

graphs can also be visualized in the PSSPLT tool, downloaded with PSS/E, by opening the output.out file.

There are 35 total possible graph outputs, the naming is 'graph' + the value required to obtain that output in the function psspy.chsb of the runDynSim_psseC python file [25]:

graph 1 ANGLE, machine relative rotor angle (degrees).

graph 2 PELEC, machine electrical power (pu on SBASE).

graph 3 QELEC, machine reactive power.

graph 4 ETERM, machine terminal voltage (pu).

graph 5 EFD, generator main field voltage (pu).

graph 6 PMECH, turbine mechanical power (pu on MBASE).

graph 7 SPEED, machine speed deviation from nominal (pu).

graph 8 XADIFD, machine field current (pu).

graph 9 ECOMP, voltage regulator compensated voltage (pu).

graph 10 VOTHSG, stabilizer output signal (pu).

graph 11 VREF, voltage regulator voltage setpoint (pu).

graph 12 BSFREQ, bus pu frequency deviations.

graph 13 VOLT, bus pu voltages (complex).

graph 14 voltage and angle

graph 15 flow (P).

graph 16 flow (P and Q).

graph 17 flow (MVA).

graph 18 apparent impedance (R and X).

graph 21 ITERM.

graph 22 machine apparent impedance

graph 23 VUEL, minimum excitation limiter output signal (pu).

graph 24 VOEL, maximum excitation limiter output signal (pu).

graph 25 PLOAD.

graph 26 QLOAD.

graph 27 GREF, turbine governor reference.

graph 28 LCREF, turbine load control reference.

graph 29 WVLCTY, wind velocity (m/s).

graph 30 WTRBSP, wind turbine rotor speed deviation (pu).

graph 31 WPITCH, pitch angle (degrees).

graph 32 WAEROT, aerodynamic torque (pu on MBASE).

graph 33 WROTRV, rotor voltage (pu on MBASE).

graph 34 WROTRI, rotor current (pu on MBASE).

graph 35 WPCMND, active power command from wind control (pu on MBASE).

graph 36 WQCMND, reactive power command from wind control (pu on MBASE).

graph 37 WAUXSG, output of wind auxiliary control (pu on MBASE).

There will be some other dynamic files, a conec and conet .flx files and a compile file. Alongside these files a PSS/E .SAV file with the converted AC grid will appear.

Chapter 5

Illustrative example

5.1 Introduction

In this chapter the model will be put to test. The intent is to prove the functionality as well as providing a base case example any user can follow as a 'tutorial' as part of the User Guide. First the AC base grid will be explained. Then, the steady-state model will be executed with 2 HVDC-VSC Multi-terminal grids included, followed by a dynamic simulation of a 100ms bus fault.

5.2 Base Case - Kundur System

The AC grid that will be employed as a base case is the Kundur System. This grid was selected because it is a well-known benchmark system used in power system stability studies. It consists of a simplified representation of a multi-machine power system with four synchronous generators connected to the main grid via transformers, two loads and a simple transmission grid. This system comes from a case example used by the power system engineer Prabha Kundur, author of 'Power System Stability and Control' [2].

The following single-line diagram shows the base Kundur System.

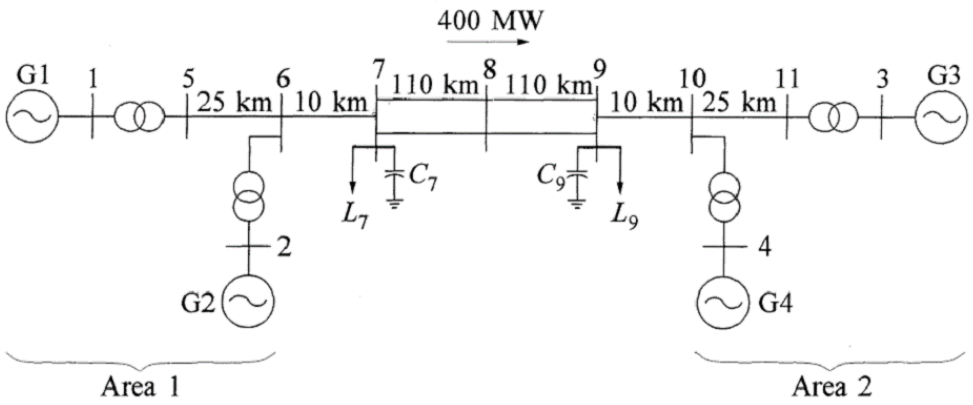

Figure 5.1: Base Kundur System

5.3 Steady-state study

This section will show how the steady-state simulation takes place alongside the results. As mentioned above the base case is the Kundur System, to which 2 Multi-terminal HVDC VSC grids are included to help with the power distribution. Firstly, the grid of study will be explained alongside its key parameters. Then, the simulation results will be provided and reflected upon.

5.3.1 HVDC-VSC Multi-terminal grid

Grid

The grid to be simulated is the simple base case Kundur System with 2 Multi-terminal HVDC VSC grids. The first one, grid A, will be connected to AC nodes 5, 7 and 11, with node 5 being the DC slack node for this grid. The second one, grid B, is connected to AC nodes 6,8 and 10, with node 6 being the DC slack node for this grid.

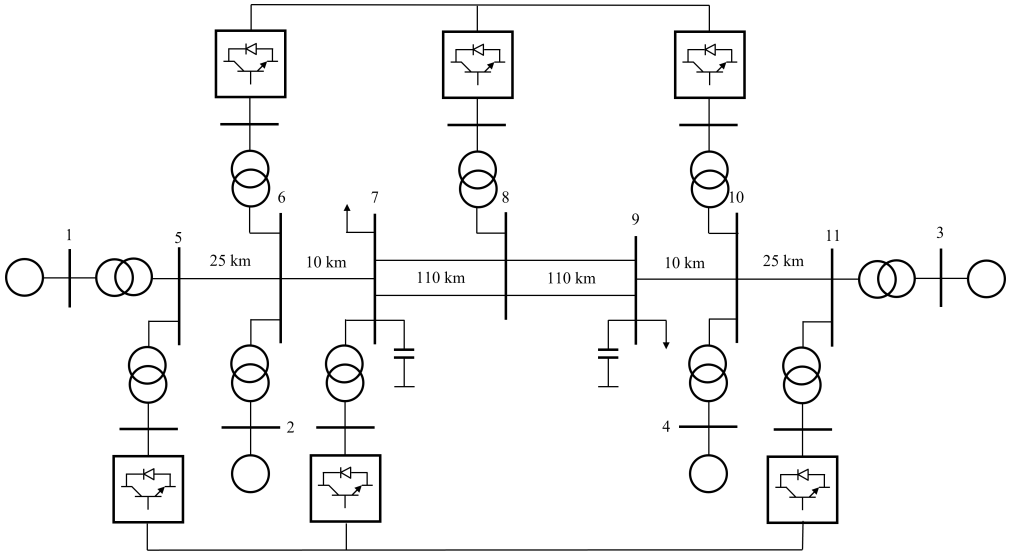

Figure 5.2: Kundur System with 2 Multi-Terminal HVDC-VSC grids

Parameters

The key parameters used for the Steady-state simulation are the following. Input of 90 MW to the first DC grid at bus 6 and an output of 45 MW on buses 8 and 10. Input of 90 MW to the second DC grid at bus 5 and an output of 45 MW on buses 7 and 11. For the converters 220 kV and 100 MVA transformers with a resistance of 0.002 pu and reactance of 0.20 pu. For the DC transmission lines the resistance is of 0.1 Ohm/km, an inductance of 0.002 H/km and a capacitance of 22 nF/km. The rest of the parameters used are included in Appendix B.

5.3.2 Results

Next, the main steady state simulation results will be displayed and commented on.

The following table presents the steady state results for the DC grid at each bus. Dctype variables determine if the bus is a DC-slack bus. We can see that the power values are the specified inputs and outputs to the DC grid. The bus numbers are the DC ones, so translated to the AC side buses they would be:
1,2,3 → 5,7,11 and 4,5,6 → 6,8,10

dcbus	dctype1	dctype2	us (p.u)	delta_s (deg)	Ps (MW)	Qs (Mvar)	udc (p.u)	Pdc (MW)
1	2	1	1.0139	6.89	−100.11	0.00	1.0000	96.69
2	1	1	0.9874	−8.52	45.00	0.00	0.9950	−47.83
3	1	1	1.0100	−6.63	45.00	0.00	0.9837	−47.83
4	2	1	0.9948	−1.58	−100.45	0.00	1.0000	97.20
5	1	1	0.9848	−16.80	45.00	0.00	0.9849	−47.79
6	1	1	0.9889	−17.61	45.00	0.00	0.9819	−47.79

Table 5.1: DC grid data for each bus

The next table shows the steady-state results for each of the branches in the Dc grid. The information displayed is the power and currents on each branch.

dc From bus	dc To bus	Pdc: ij (MW)	Pdc: ji (MW)	Icc: ij (p.u)
1	2	69.48	−69.13	0.6948
1	3	27.21	−26.77	0.2721
2	3	21.30	−21.06	0.2141
4	5	60.73	−59.82	0.6073
4	6	36.47	−35.81	0.3647
5	6	12.02	−11.98	0.1221

Table 5.2: DC grid data for each branch

The next table shows the converter loses divided into the loses of the transformer, reactor and VSC.

transformer	reactor	VSC converters losses	total Coupling AC/DC
0.1950	0.3899	2.83	3.41
0.0415	0.0831	2.71	2.83
0.0397	0.0794	2.71	2.83
0.0102	0.4078	2.83	3.25
0.0021	0.0835	2.71	2.79
0.0021	0.0828	2.71	2.79

Table 5.3: VSC converters - losses (MW) and AC/DC coupling

The total Active Power loss for the AC/DC coupling is the sum of the final column. Which gives a result, to 2 decimal places, of: 17.91 MW

	Base Case Kundur	Multi-Terminal HVDC VSC Case
PSS/E Losses Report (MW)	85.1	69.4
AC/DC Coupling Losses (MW)	0.0	17.9
Total (MW)	85.1	87.3

(a) Active Power Losses Comparison

	Base Case Kundur	Multi-Terminal HVDC VSC Case
PSS/E Losses Report (Mvar)	1193.3	1027.3
AC/DC Coupling Losses (Mvar)	0.0	0.0
Total (Mvar)	1193.3	1027.3

(b) Reactive Power Losses Comparison

	Base Case Kundur	Multi-Terminal HVDC VSC Case
PSS/E Losses Report (MVA)	1196.3	1029.6
AC/DC Coupling Losses (MVA)	0.0	17.9
Total (MVA)	1196.3	1031.0

(c) Power Losses Comparison

The results show that with the implementation of the VSC - HVDC Multi-Terminal grids, there is an increased loss of 3% in MW but a total decrease of 14% in MVA.

The next table shows the steady-state results of the converters operating point.

ec (p.u)	delta_c (deg)	Pc (MW)	Qc (Mvar)
1.0355	−6.34	−99.52	23.40
0.9962	−2.22	45.12	4.98
1.0183	−0.61	45.12	4.76
0.9915	−3.92	−100.03	4.09
0.9869	−15.73	45.09	0.84
0.9909	−16.56	45.08	0.83

Table 5.5: VSC Converters Operating Point

5.4 Dynamic Simulation

This section will demonstrate the capability of the simulation program to dynamically study 2 Multi-terminal HVDC VSC grids. Once again, these grids will be included into the same Kundur base case. As in other chapters on the dynamic model, the main focus of this section is to commentate on the dynamic results, but prior to this study a steady-state has to be performed, as the results are used to initialize the dynamic simulation. Therefore, to avoid repetition and stick to the main focus of the section, the steady-state part will be less thorough. Firstly, the grid of study will be explained alongside its key parameters. Then, the simulation results will be provided and reflected upon.

5.4.1 HVDC-VSC Multi-terminal grid

Parameters

The parameters for the dynamic simulation are the same as the ones for the steady-state plus some dynamic parameters that have been set to standard values, the dynamic parameters have been included in Appendix C. The simulated event is a bus fault of 100 ms at bus 9.

5.4.2 Results

The next plots will summarize the dynamic results obtained from the simulation. The following are some of the most important ones but there are 35 total possible graph outputs for the dynamic simulation.

The next two figures show the voltage of the converters at the buses where the VSC-HVDC Multi-Terminal grids are linked to the AC grid. The first grid, Figure 5.3, shows buses 6, 8 and 10 and the second grid, Figure 5.4, shows buses 5, 7 and 11. It is observed that the voltage decreases more at the converters closer to the fault and less at those further away from the fault. Afterwards, the voltage levels are restored satisfactorily.

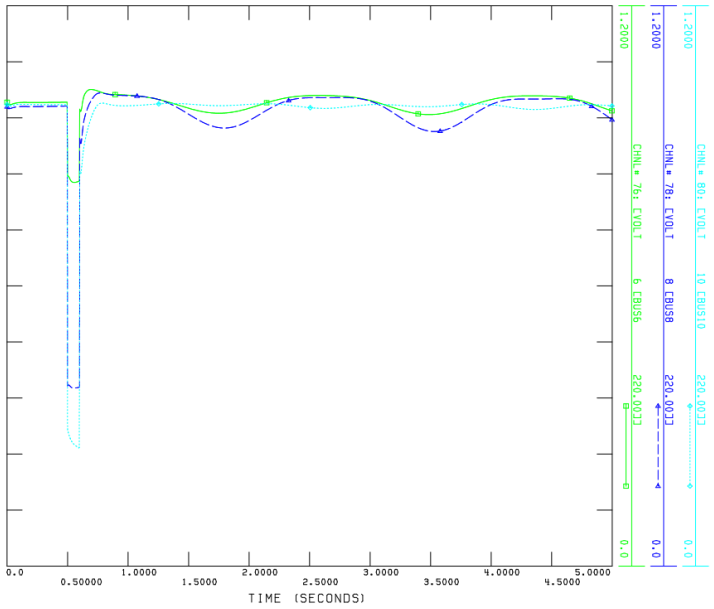

Figure 5.3: Voltage of converters at buses 6, 8 and 10 - Grid 1

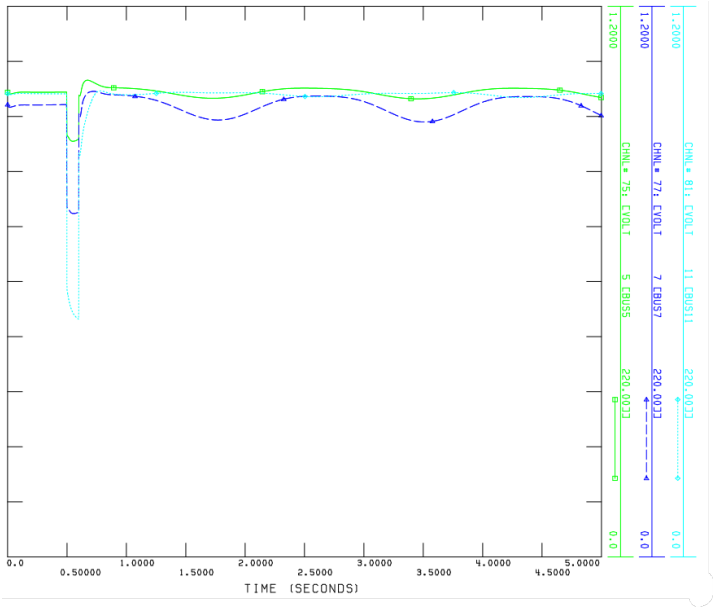

Figure 5.4: Voltage of converters at buses 5, 7 and 11 - Grid 2

The next two figures show the active power at the converter buses. The first grid, Figure 5.3, shows buses 6, 8 and 10 and the second grid, Figure 5.4, shows buses 5, 7 and 11. It is observed that the active power response is rapid then, the

pre-fault values are restored. Once more the largest difference occurs at the buses closest to the fault.

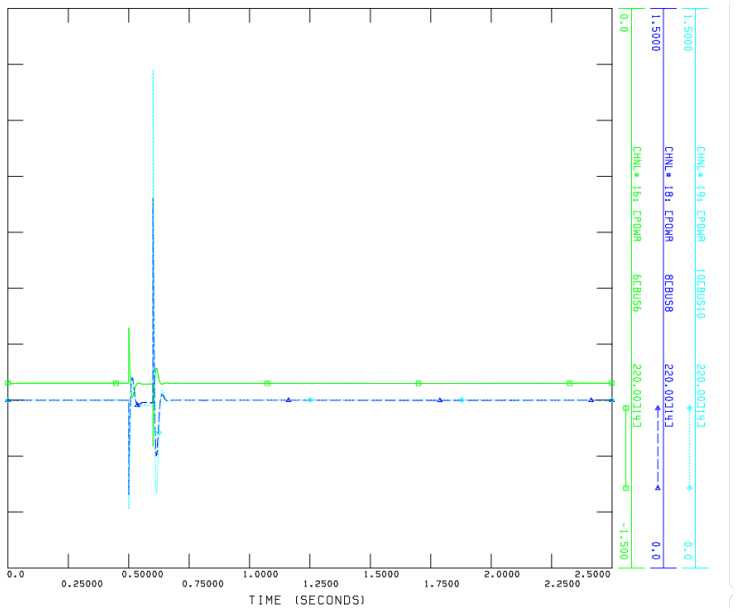

Figure 5.5: Active Power at buses 6, 8 and 10 - Grid 1

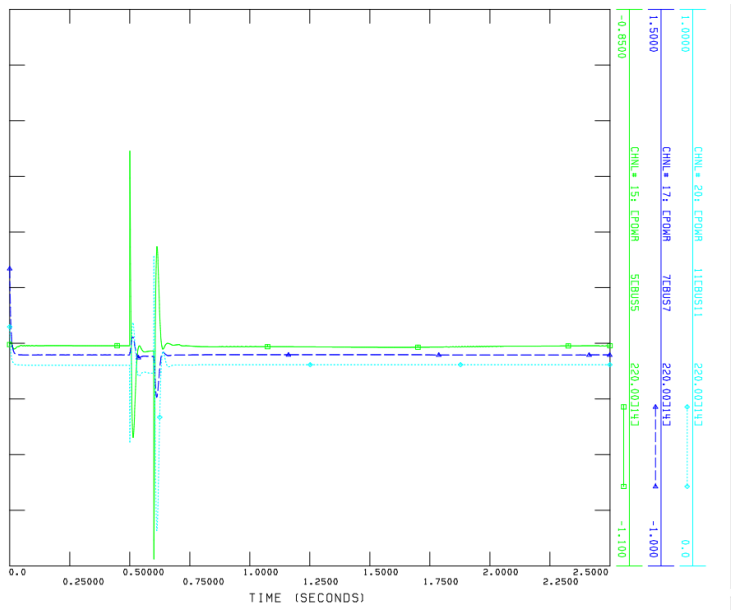

Figure 5.6: Active Power at buses 5, 7 and 11 - Grid 2

The next two figures show the reactive power at the converter buses. The

first grid, Figure 5.3, shows buses 6, 8 and 10 and the second grid, Figure 5.4, shows buses 5, 7 and 11. It is observed that the reactive power response is rapid. The reactive power involved in these buses is small, but the values are restored satisfactorily shortly after the fault disappears.

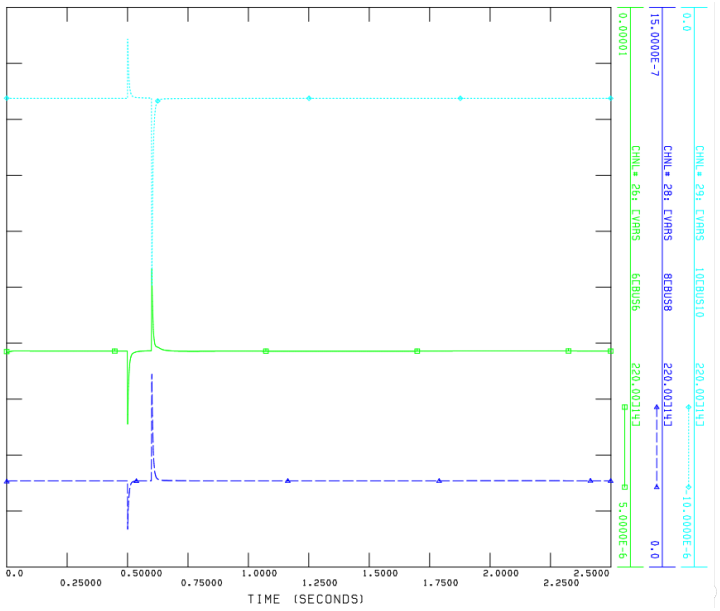

Figure 5.7: Reactive Power at buses 6, 8 and 10 - Grid 1

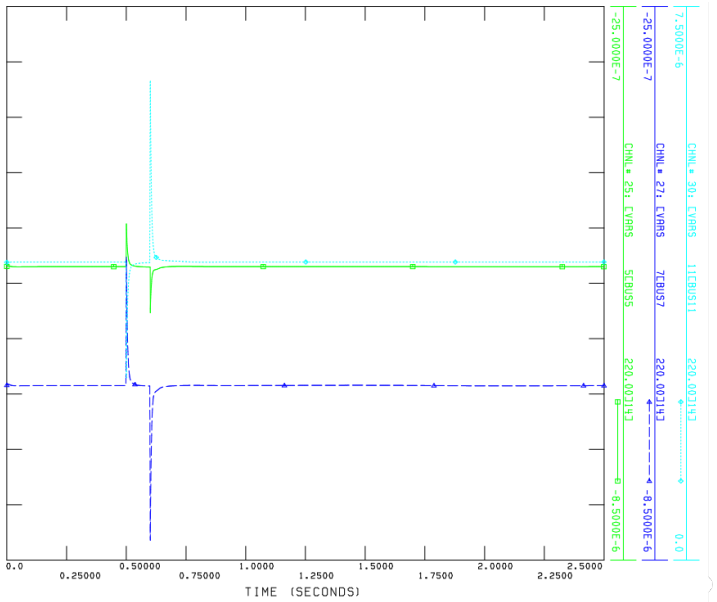

Figure 5.8: Reactive Power at buses 5, 7 and 11 - Grid 2

The next figures show the frequency of the system for the base case, Figure 5.10, and for the VSC-HVDC Multi-Terminal case, Figure 5.9. The fault splits the AC grid in 2 but the Multi-Terminal HVDC grid connecting the 2 areas makes the restoring of the frequency more effective. In the base case the frequency isn't restored after 5 s but it is when the Multi-Terminal HVDC grids are in place. Proving that the inclusion of such grids increases the stability of the system against faults.

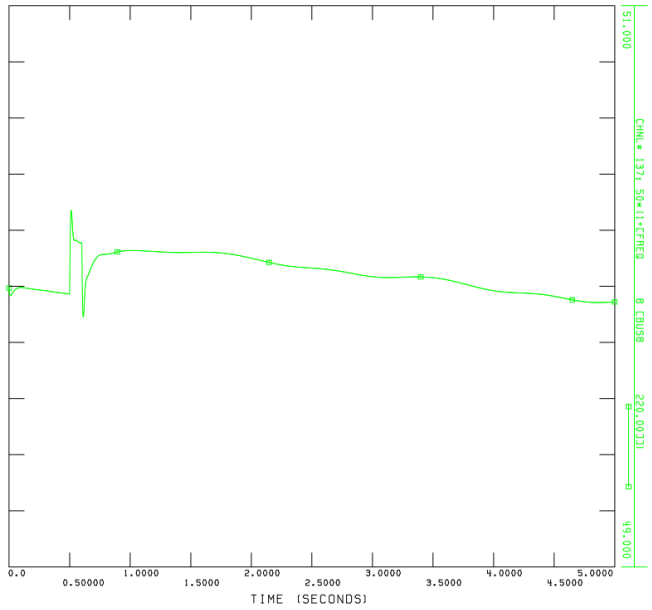

Figure 5.9: Frequency of the system, with VSC-HVDC Multi-Terminal grids.

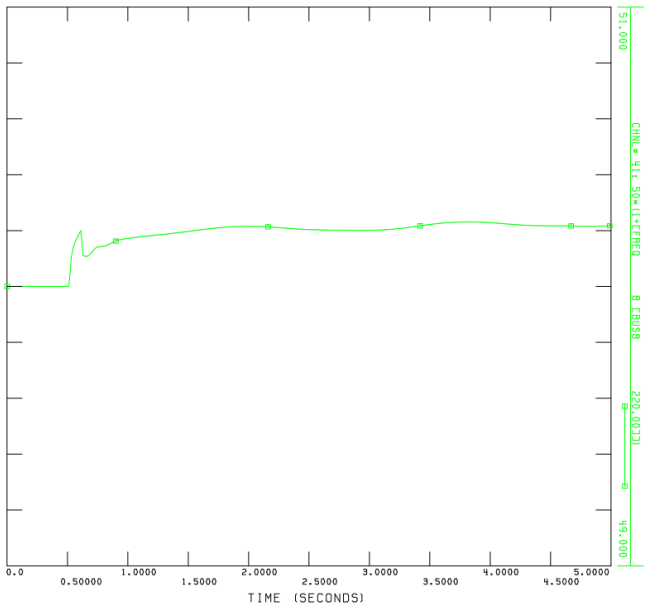

Figure 5.10: Frequency of the system, base case.

Chapter 6

Conclusion

This chapter will act as a summary, organising the main results and implications alongside the some proposals for future research. But firstly, a refreshment on the aim of this thesis will be included to comment on the achievement of such objective without overseeing the limitations there are.

The main topic of the work was High Voltage Direct Current interconnections. Links which offer serious advantages for specific use cases such as: bulk energy transfer over long distances at lower losses, asynchronous connections of regions even when they are of different frequencies, reduced losses for underground / underwater connections and reduced rights of way.

Some notable examples being the Gotland project, the Peninsula-Baleares link, the Itaipu inter-frequency link, the Quebec-New England- New York Multi-Terminal HVDC grid. To re-state some.

These advantages make it the preferred option for certain applications. HVDC has been successfully integrated in many instances, more so in recent years as previously the non-existence of an effective DC breaker limited its growth. It was the introduction of these, alongside many other milestones, what caused a surge in the interest of further developing these single point-to-point links into Multi-Terminal HVDC grids.

Furthermore, the two main converter technologies being used are LCC and VSC. Whilst VSC, the newer technology, has some advantages over LCC there is no Multi-Terminal HVDC-VSC simulation tools. In order to exploit such advantages, a simulation model was to be created.

IIT has developed a model to simulate Multi-Terminal HVDC-VSC grids. But, there is an industrial desire to extend this model to enable multiple of these grids

to be simulated at once. Therefore, the key objective of this work was to extend both the steady state and dynamic models to enable the simulation of a multitude of Multi-Terminal HVDC-VSC grids. Being offshore wind farm connection to the mainland grids in California and the North Sea some of the first sectors to require such a model.

After this work, a PSS/E model for the simulation of multiple HVDC-VSC Multi-Terminal grids has been developed. The results commented on Chapter 5 are the expected of such a grid. It can be seen that for the Kundur base case, the introduction of both HVDC-VSC reduces the power losses and due to the reactive power involved in the link, the MVA produced to meet the demand decreased by 14%. Dynamically, it is concluded that VSC technology allows for a satisfactory and rapid restoration of pre-fault values, specially in the active and reactive power values. Proving another of the advantages, increased grid stability.

The simulation tool developed is not all encompassing and has some limitations. For the steady state model convergence is not granted, it depends on initial conditions, as in any iteration based power flow tool. The AC grid must not have generators identified as being from area '14', as this is the identifier used for HVDC converters. The PSS/E version used in conjunction with the model will offer its own set of limitations. For the dynamic model, currently, a Fortran compiler is required every time the steady state output files are relocated to a different folder, as the path is hard coded into the Fortran file.

As future recommendations when further developing this model, some limitations are avoidable and should be corrected. The HVDC identifier should be a user input and the Fortran file should be updated to obtain automatically its current working directory.

Other future recommendations, detached from these limitations, is the creation of a model for the economic viability study of such grids that uses the simulation tool here developed. It could be interesting to study, cost wise, the advantages of expanding simple HVDC links to Multi-Terminals or the economic feasibility of some proposed projects such as North Sea HVDC grid or a European Supergrid.

Appendix A

SDG

The SDGs, Sustainable Development Goals, are a set of 17 goals created by the United Nations in order to provide a guide for peace, prosperity and sustainability of the human race. With an independence on the project or decision made, it could be argued that if it follows these blueprints, this project would be socially desirable.

As mentioned in the previous subsection these grids are helpful for the introduction of renewable sources of energy, increasing the sustainability of the electric network. But, prior to the physical implementation of these HVDC VSC grids a simulation tool must be developed so that a study can be carried, aligning this project with both Goal 7 (Affordable and Clean Energy) and Goal 11 (Sustainable cities and communities). Also, due to the industrial nature of this thesis, Goal 9 (Industry, innovation and infrastructure) is also worked upon.

Appendix B

Steady-state parameters illustrative example

These are the parameters used in the steady-state model for the illustrative example:

First Multi-Terminal HVDC-VSC grid connected at buses 5, 7 and 11.

system MVA base = 100.0

converters and AC/DC coupling data:
from DC bus, to AC bus, rt, xt, bf, rc, xc, a, b, crect, cinv, Pmax, Pmin, Qmax, Qmin, rateA, rateB, rateC, ratio, angle, status, angmin, angmax

ppc["converter"] = array([

[1, 5, 0.002, 0.2, 0.0000, 0.004, 0.04, $26.25*e^{-3}$, $1.65*e^{-3}$, $4.2*e^{-4}$, $6.28*e^{-4}$, 9999, -9999, 999, -999, 500, 0, 0, 0, 0, 1, -360, 360],

[2, 7, 0.002, 0.2, 0.0000, 0.004, 0.04, $26.25*e^{-3}$, $1.65*e^{-3}$, $4.2*e^{-4}$, $6.28*e^{-4}$, 9999, -9999, 999, -999, 500, 0, 0, 0, 0, 1, -360, 360],

[3, 11, 0.002, 0.2, 0.0000, 0.004, 0.04, $26.25*e^{-3}$, $1.65*e^{-3}$, $4.2*e^{-4}$, $6.28*e^{-4}$, 9999, -9999, 999, -999, 500, 0, 0, 0, 0, 1, -360, 360],

])

DC bus data
bus_i, type1 (1: node P, 2: dc-slack), type2 (1: control of Qs, 2: control of u_s), Us,

$delta_s$, Ps, Qs, Udc, Pdc, iny, Idc, Gdc, Cdc, area, baseKV, zone, Vmax, Vmin

ppc["dcbus"] = array([

[1, 2, 1, 1.00, 0, -90, 0.0, 1.00, 0, 0, 0, 0.39936, 1, 220, 1, 1.06, 0.94],

[2, 1, 1, 1.00, 0, 45, 0.0, 1.00, 0, 0, 0, 0.39936, 1, 220, 1, 1.06, 0.94],

[3, 1, 1, 1.00, 0, 45, 0.0, 1.00, 0, 0, 0, 0.39936, 1, 220, 1, 1.06, 0.94],

])

DC branch data
from bus, to bus, r, Ldc, Ccc, rateA, rateB, rateC, ratio, angle, status

ppc["dcbranch"] = array([

[1, 2, $2.06612*1e^{-4}*$ 35.0, $1.2981788*1e^{-4}*$ 35.0, $3.34517*1e^{-4}*$ 35.0, 1000, 0, 0, 0, 0, 1, 0, 0, 0],

[1, 3, $2.06612*1e^{-4}*$ 290.0, $1.2981788*1e^{-4}*$ 290.0, $3.34517*1e^{-4}*$ 290.0, 1000, 0, 0, 0, 0, 1, 0, 0, 0],

[2, 3, $2.06612*1e^{-4}*$ 255.0, $1.2981788*1e^{-4}*$ 255.0, $3.34517*1e^{-4}*$ 255.0, 1000, 0, 0, 0, 0, 1, 0, 0, 0],

])

Second Multi-Terminal HVDC-VSC grid connected at buses 6, 8 and 10.

system MVA base = 100.0

converters and AC/DC coupling data:
from DC bus, to AC bus, rt, xt, bf, rc, xc, a, b, crect, cinv, Pmax, Pmin, Qmax, Qmin, rateA, rateB, rateC, ratio, angle, status, angmin, angmax

ppc["converter"] = array([

[4, 6, 0.0001, 0.0001, 0.0000, 0.004, 0.04, 26.25e-3, 1.65e-3, 4.2e-4, 6.28e-4, 9999, -9999, 999, -999, 500, 0, 0, 0, 0, 1, -360, 360],

[5, 8, 0.0001, 0.0001, 0.0000, 0.004, 0.04, 26.25e-3, 1.65e-3, 4.2e-4, 6.28e-4, 9999, -9999, 999, -999, 500, 0, 0, 0, 0, 1, -360, 360],

[6, 10, 0.0001, 0.0001, 0.0000, 0.004, 0.04, 26.25e-3, 1.65e-3, 4.2e-4, 6.28e-4, 9999, -9999, 999, -999, 500, 0, 0, 0, 0, 1, -360, 360],

])

DC bus data

bus_i, type1 (1: node P, 2: dc-slack), type2 (1: control of Qs, 2: control of u_s), Us, $delta_s$, Ps, Qs, Udc, Pdc, iny, Idc, Gdc, Cdc, area, baseKV, zone, Vmax, Vmin

ppc["dcbus"] = array([

[4, 2, 1, 1.00, 0, -90, 0.0, 1.00, 0, 0, 0, 0.39936, 1, 220, 1, 1.06, 0.94],

[5, 1, 1, 1.00, 0, 45, 0.0, 1.00, 0, 0, 0, 0.39936, 1, 220, 1, 1.06, 0.94],

[6, 1, 1, 1.00, 0, 45, 0.0, 1.00, 0, 0, 0, 0.39936, 1, 220, 1, 1.06, 0.94]

])

DC branch data

from bus, to bus, r, Ldc, Ccc, rateA, rateB, rateC, ratio, angle, status

ppc["dcbranch"] = array([

[4, 5, $2.06612*1e^{-4}*$ 120.0, $1.2981788*1e^{-4}*$ 120.0, $3.34517*1e^{-4}*$ 120.0, 1000, 0, 0, 0, 0, 1, 0, 0, 0],

[4, 6, $2.06612*1e^{-4}*$ 240.0, $1.2981788*1e^{-4}*$ 240.0, $3.34517*1e^{-4}*$ 240.0, 1000, 0, 0, 0, 0, 1, 0, 0, 0],

[5, 6, $2.06612*1e^{-4}*$ 120.0, $1.2981788*1e^{-4}*$ 120.0, $3.34517*1e^{-4}*$ 120.0, 1000, 0, 0, 0, 0, 1, 0, 0, 0]

])

Appendix C

Dynamic parameters illustrative example

These are the parameters used in the dynamic model for the illustrative example (the steady-state parameters on Appendix B still apply):

/Dynamic Data

/NODE1
1 'GENROU' 1 8 0.03 0.4 0.05 6.5 0 1.8 1.7 0.3 0.55 0.25 0.2 0.0435 0.2963 /
1 'EXST1' 1 0.01 1.0 -1.0 0.0 0.0 200 0.0 6.4 -6.4 0.1 0 1.0 /
/ 1 'STAB1' 1 20 10 2.5 0.02 0.5555 5.4 0.05 /
/ 1 'IEEEG1' 1 0 0 20.0 0 0 0.3 1.0 -1.0 1.0 -1.0 0.3 0.3 0.0 7.0 0.3 0.0 0.6 0.4 0.0 0.0 0.0 0.0 /

/NODE2
2 'GENROU' 1 8 0.03 0.4 0.05 6.5 0 1.8 1.7 0.3 0.55 0.25 0.2 0.0435 0.2963 /
2 'EXST1' 1 0.01 1.0 -1.0 0.0 0.0 200 0.0 6.4 -6.4 0.1 0 1.0 /
/ 2 'STAB1' 1 20 10 2.5 0.02 0.5555 5.4 0.05 /
/ 2 'IEEEG1' 1 0 0 20.0 0 0 0.3 1.0 -1.0 1.0 -1.0 0.3 0.3 0.0 7.0 0.3 0.0 0.6 0.4 0.0 0.0 0.0 0.0 /

/NODE3
3 'GENROU' 1 8 0.03 0.4 0.05 6.5 0 1.8 1.7 0.3 0.55 0.25 0.2 0.0435 0.2963 /
3 'EXST1' 1 0.01 1.0 -1.0 0.0 0.0 200 0.0 6.4 -6.4 0.1 0 1.0 /
/ 3 'STAB1' 1 20 10 2.5 0.02 0.5555 5.4 0.05 /
/ 3 'IEEEG1' 1 0 0 20.0 0 0 0.3 1.0 -1.0 1.0 -1.0 0.3 0.3 0.0 7.0 0.3 0.0 0.6 0.4 0.0 0.0 0.0 0.0 /

/NODE4

4 'GENROU' 1 8 0.03 0.4 0.05 6.5 0 1.8 1.7 0.3 0.55 0.25 0.2 0.0435 0.2963 /
4 'EXST1' 1 0.01 1.0 -1.0 0.0 0.0 200 0.0 6.4 -6.4 0.1 0 1.0 /
/ 4 'STAB1' 1 20 10 2.5 0.02 0.5555 5.4 0.05 /
/ 4 'IEEEG1' 1 0 0 20.0 0 0 0.3 1.0 -1.0 1.0 -1.0 0.3 0.3 0.0 7.0 0.3 0.0 0.6 0.4 0.0 0.0 0.0 0.0 /

/ VSC-HVDC Multi-terminal

/ bus 5 - converter
5 'USRMDL' 14 'SVSCON' 1 1 7 24 7 33 1 1 1 1 3 'A' 0 0.005 0.00 0.0 20.0 1.2 0.0 0.0 0.0 150.0 3000.0 1.00 500 -500 200 -200 1.10 0.90 1.31 2.625 0.6287 0.2033 0.3040 195.00 220 //
5 'USRMDL' 14 'SPWDRD' 4 0 3 12 3 15 1 0 0 0.100 10.0 0.1 200.0 10.0 0.00001 0.00001 0.0001 1.0 -1.0 999.45 0.2 /
5 'USRMDL' 14 'SQWDRD' 3 0 3 13 3 14 0 0 0 0.100 10.0 0.1 200.0 10.0 0.00001 0.00001 0.0001 0.4 -0.4 999.45 1.5 9999.0 /
5 'USRMDL' 14 'DCGRID' 5 0 8 2 6 6 3 3 2 'A' 6 6 0 0 220 100/
5 'USRMDL' 14 'WDELAY' 9 0 6 5 8 6 1 4 5 6 11 10 0.000 0.000 0.000 0.000 0.000 /

/ bus 7 - converter
7 'USRMDL' 14 'SVSCON' 1 1 7 24 7 33 2 1 1 1 3 'A' 0 0.005 0.00 0.0 20.0 1.2 0.0 0.0 0.0 150.0 3000.0 1.00 500 -500 200 -200 1.10 0.90 1.31 2.625 0.6287 0.2033 0.3040 195.00 220 //
7 'USRMDL' 14 'SPWDRD' 4 0 3 12 3 15 1 0 0 0.100 10.0 0.1 200.0 10.0 0.00001 0.00001 0.0001 1.0 -1.0 999.45 0.2 /
7 'USRMDL' 14 'SQWDRD' 3 0 3 13 3 14 0 0 0 0.100 10.0 0.1 200.0 10.0 0.00001 0.00001 0.0001 0.4 -0.4 999.45 1.5 9999.0 /
7 'USRMDL' 14 'WDELAY' 9 0 6 5 8 6 1 4 5 6 11 10 0.000 0.000 0.000 0.000 0.000 /

/ bus 11 - converter
11 'USRMDL' 14 'SVSCON' 1 1 7 24 7 33 3 1 1 1 3 'A' 0 0.005 0.00 0.0 20.0 1.2 0.0 0.0 0.0 150.0 3000.0 1.00 500 -500 200 -200 1.10 0.90 1.31 2.625 0.6287 0.2033 0.3040 195.00 220 //
11 'USRMDL' 14 'SPWDRD' 4 0 3 12 3 15 1 0 0 0.100 10.0 0.1 200.0 10.0 0.00001 0.00001 0.0001 1.0 -1.0 999.45 0.2 /
11 'USRMDL' 14 'SQWDRD' 3 0 3 13 3 14 0 0 0 0.100 10.0 0.1 200.0 10.0 0.00001 0.00001 0.0001 0.4 -0.4 999.45 1.5 9999.0 /
11 'USRMDL' 14 'WDELAY' 9 0 6 5 8 6 1 4 5 6 11 10 0.000 0.000 0.000 0.000 0.000 /

/ bus 6 - converter
6 'USRMDL' 14 'SVSCON' 1 1 7 24 7 33 4 1 1 1 3 'B' 3 0.005 0.00 0.0 20.0 1.2
0.0 0.0 0.0 150.0 3000.0 1.00 500 -500 200 -200 1.10 0.90 1.31 2.625 0.6287 0.2033
0.3040 195.00 220 //
6 'USRMDL' 14 'SPWDRD' 4 0 3 12 3 15 1 0 0 0.100 10.0 0.1 200.0 10.0 0.00001
0.00001 0.0001 1.0 -1.0 999.45 0.2 /
6 'USRMDL' 14 'SQWDRD' 3 0 3 13 3 14 0 0 0 0.100 10.0 0.1 200.0 10.0 0.00001
0.00001 0.0001 0.4 -0.4 999.45 1.5 9999.0 /
6 'USRMDL' 14 'DCGRID' 5 0 8 2 6 6 3 3 2 'B' 6 6 3 3 220 100/
6 'USRMDL' 14 'WDELAY' 9 0 6 5 8 6 1 4 5 6 11 10 0.000 0.000 0.000 0.000 0.000
/

/ bus 8 - converter
8 'USRMDL' 14 'SVSCON' 1 1 7 24 7 33 5 1 1 1 3 'B' 3 0.005 0.00 0.0 20.0 1.2
0.0 0.0 0.0 150.0 3000.0 1.00 500 -500 200 -200 1.10 0.90 1.31 2.625 0.6287 0.2033
0.3040 195.00 220 //
8 'USRMDL' 14 'SPWDRD' 4 0 3 12 3 15 1 0 0 0.100 10.0 0.1 200.0 10.0 0.00001
0.00001 0.0001 1.0 -1.0 999.45 0.2 /
8 'USRMDL' 14 'SQWDRD' 3 0 3 13 3 14 0 0 0 0.100 10.0 0.1 200.0 10.0 0.00001
0.00001 0.0001 0.4 -0.4 999.45 1.5 9999.0 /
8 'USRMDL' 14 'WDELAY' 9 0 6 5 8 6 1 4 5 6 11 10 0.000 0.000 0.000 0.000 0.000
/

/ bus 10 - converter
10 'USRMDL' 14 'SVSCON' 1 1 7 24 7 33 6 1 1 1 3 'B' 3 0.005 0.00 0.0 20.0 1.2
0.0 0.0 0.0 150.0 3000.0 1.00 500 -500 200 -200 1.10 0.90 1.31 2.625 0.6287 0.2033
0.3040 195.00 220 //
10 'USRMDL' 14 'SPWDRD' 4 0 3 12 3 15 1 0 0 0.100 10.0 0.1 200.0 10.0 0.00001
0.00001 0.0001 1.0 -1.0 999.45 0.2 /
10 'USRMDL' 14 'SQWDRD' 3 0 3 13 3 14 0 0 0 0.100 10.0 0.1 200.0 10.0 0.00001
0.00001 0.0001 0.4 -0.4 999.45 1.5 9999.0 /
10 'USRMDL' 14 'WDELAY' 9 0 6 5 8 6 1 4 5 6 11 10 0.000 0.000 0.000 0.000
0.000 /

Bibliography

[1] Javier Renedo, Aurelio García-Cerrada, Luis Rouco, Lukas Sigrist, Ignacio Egido, and Silvia Sanz Verdugo. Development of a pss/e tool for power-flow calculation and dynamic simulation of vsc-hvdc multi-terminal systems. 2017.

[2] Prahba Kundur. *Power System Stability and Control*. McGraw Hill Education, 1993.

[3] Kerstin Lindén and Peter Lundberg. Multi-terminal webinar presentation. 2021.

[4] Per Skarby. ABB review special report 60 years of HVDC. Technical report, ABB, 2014.

[5] Mojtabba Mohaddes. Introduction to hvdc. In *Tutorial sponsored by Study Committee B4, Cigre Session 46, Paris, France*, 21-26 August 2016.

[6] Francisco Javier Renedo Anglada. Control of VSC-HVDC multi-terminal systems to improve angle stability in hybrid HVAC/HVDC electrical transmission systems. 2018.

[7] Stamatiou Georgios. *Techno-Economical Analysis of DC Collection Grid for Offshore Wind Parks*. Master's thesis, University of Nottingham, 2010.

[8] Summit: North Sea Energy Cooperation. Ostend declaration on the north seas as europe's green power plant, 2022.

[9] G. Buigues, V. Valverde, Agurtzane Etxegarai, Pablo Eguia, and E. Torres. Present and future multiterminal hvdc systems: current status and forthcoming. *Renewable Energy and Power Quality Journal*, 1:83–88, 04 2017.

[10] Atsushi Nishioka, Fidel Alvarez, and Takahiro Omori. Global rise of hvdc and its background. Technical report, Global Innovation Report Hitachi ABB, 2020.

[11] Magnus Callavik, Peter Lundberg, Jürgen Häfner, Hans Björklund, Munaf Rahimo, and Franc Dugal. Evolution of hvdc light. Technical report, ABB REVIEW, 2018.

[12] Hitachi ABB. The gotland hvdc link. *Website Report*, 2023.

[13] Hitachi ABB Energy Report. 'the first large-scale multi-terminal hvdc transmission in the world', 2022.

[14] Red Eléctrica de España. Rómulo, Interconexión Eléctrica Península-Baleares. Technical report, REE, 2011.

[15] Mike Barnes and Antony Beddard. *Voltage Source Converter HVDC Links – The state of the Art and Issues Going Forward*. Master's thesis, University of Manchester, 2012.

[16] Stijn Cole, Jef Beerten, and Ronnie Belmans. Generalized Dynamic VSC MTDC Model for Power System Stability Studies. *IEEE Transactions on Power Systems*, 25(3):1655–1662, 2010.

[17] G. Daelemans. *VSC HVDC in meshed networks*. Master's thesis, Katholieke Universiteit Leuven, 2008.

[18] Jef Beerten, Stijn Cole, and Ronnie Belmans. Generalized Steady-State VSC MTDC Model for Sequential AC / DC Power Flow Algorithms. *IEEE Transactions on Power Systems*, 27(2):821–829, 2012.

[19] Federico Milano. *Power System Modelling and Scripting*. Springer, 2010.

[20] Jef Beerten, Oriol Gomis-Bellmunt, Xavier Guillaud, Johan Rimez, Arjen van der Meer, and Dirk Van Hertem. Modeling and control of HVDC grids: a key challenge for the future power system. In *PSCC*, pages 1–21, 2014.

[21] P. J. D Chainho. *General Modeling of Multi-Terminal VSC-HVDC Systems for Transient Stability Analysis*. Master's thesis, Universidade Técnica de Lisboa, 2012.

[22] Jef Beerten, Stijn Cole, and Ronnie Belmans. Modeling of Multi-Terminal VSC HVDC Systems With Distributed DC Voltage Control. *IEEE Transactions on Power Systems*, 29(1):34–42, 2014.

[23] Javier Renedo, Aurelio García-Cerrada, and Luis Rouco. Active Power Control Strategies for Transient Stability Enhancement of AC/DC Grids With VSC-HVDC Multi-Terminal Systems. *IEEE Transactions on Power Systems*, 31(6):4595–4604, 2016.

[24] Siemens-PTI. *PSS/E 30.2 Program Operation Manual*, volume 2. 2005.

[25] Siemens-PTI. *PSS/E 34.3 Application Program Interface*, volume 1. 2017.